Award Number: 02HQGR0055

IDENTIFYING FAULTS AND THIER RECENT MOTION IN EASTERN STRAIT OF JUAN DE FUCA.

Calvert, A., Hayward, N., Nedimovic, M., and Cleary, M.

Earth Sciences,
Simon Fraser University
8888 University Drive,
Burnaby, B.C.
V5A 1S6
CANADA

phone: (604) 291 5511
fax: (604) 291 4198
e-mail: acalvert@sfu.ca

Abstract

Award Number: 02HQGR0055

IDENTIFYING FAULTS AND THIER RECENT MOTION IN EASTERN STRAIT OF JUAN DE FUCA.

Calvert, A., Hayward, N., Nedimovic, M., and Cleary, M.

Earth Sciences, Simon Fraser University,
8888 University Drive, Burnaby, B.C. V5A 1S6 CANADA
phone: (604) 291 5511 fax: (604) 291 4198 e-mail: acalvert@sfu.ca

Multi-channel seismic reflection data, acquired in the SHIPS (Seismic Hazards Investigation in Puget Sound) survey are used to interpret the faulting and structure of the eastern Strait of Juan de Fuca. A number of major fault zones, including the Devils Mountain, a left-lateral transpressional fault zone, and the Southern Whidbey Island fault zone, underlie the region of large prehistoric earthquakes. Numerous Pleistocene glaciations and associated erosion and deposition have resulted in the surface masking of faults, which are now most easily investigated using seismic data. In this study, first arrival tomographic velocity models derived from the seismic data are used to accurately characterise the shallow P-wave velocity structure across fault zones and aid in the identification of potentially active faults, which may pose a significant seismic hazard to local communities.

Seismic reflection data from SHIPS lines JDF-1-6, PS-2 and SG-1 were reprocessed, using variable shot spacing geometry, to improve the quality of seismic images and allow for more detailed interpretation of the near surface. First arrival tomographic inversion velocities were calculated using an iterative two-dimensional inversion algorithm based on a finite-difference solution to the eikonal equation. With far offsets of approximately 2600 m, a high density of subsurface raypaths and a velocity grid spacing of 25 m, a high-resolution estimate of P-wave velocity structure is calculated for depths in the range of 500-1200 m. These P-wave velocity models provide information on the variation of physical properties with depth and across faults, which when overlain directly upon seismic profiles significantly aid in the interpretation.

Seismic reflection profiles, of the Devils Mountain fault, suggest that primary pre-Quaternary motion to the east of 122.95° W was transferred to a large fault scarp identified on profiles south of the mapped E-W trend on the DMF. This fault scarp appears to be related to the westward extension on the Utsalady Point fault, which shows a similar, although slightly smaller scarp west of Whidbey Island. More recent deformation has been experienced on the eastward continuance of the DMF, which east of 122.95° W affects a shallow pre-Tertiary basement and thin overburden far north of the primary fault scarp. However, Quaternary deformation associated with the primary fault scarp appears to be of as large a magnitude as faulting on the DMF to the northeast.

1. Introduction

The Eastern Strait of Juan de Fuca (SJDF) is located to the southeast of Vancouver Island (inset, Fig. 1), on the west coast of Canada. The Juan de Fuca oceanic plate is currently subducting north-eastwards at approximately 46 mm/yr beneath Vancouver Island, resulting in stress in the overlying plate.

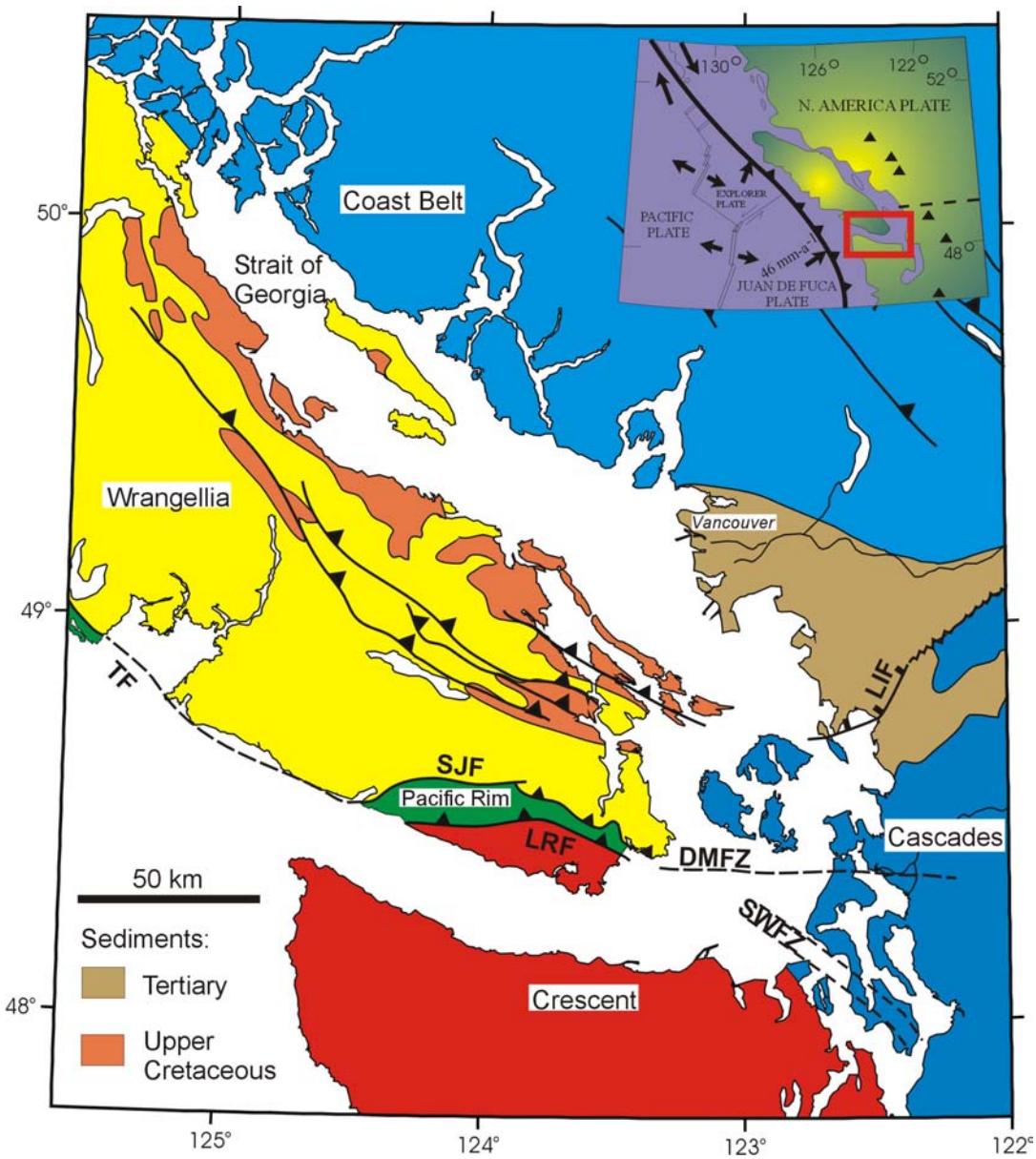

Figure 1. Location of the study region and tectonic setting. Fault Zones: DMFZ = Devils Mountain; SWFZ = Southern Whidbey Island; SJF = San Juan; LRF = Long Range. Red box on inset shows location of study region shown in figure 2.

GPS measurements (Mazzotti 2002; Miller 2001) indicate a north-south shortening rate of about 5-7 mm/yr for the inner forearc, leading to a potential for large magnitude earthquakes in a region that has experienced large prehistoric crustal earthquakes (Gower et al. 1985; Atwater and Moore 1992).

Previous investigations in the Eastern Strait of Juan de Fuca (e.g. Mosher et al. 2000; Johnson et al. 2001) have revealed a complex pattern of faulting and folding which has affected Tertiary to recent sedimentary rocks whose base represents a disconformity upon underlying pre-Tertiary basement rocks. These comprise a number of tectonic terranes (Fig. 1) that were accreted to the western Canada margin in the past. Pleistocene glaciers (Booth 1994) eroded near surface sediments and rocks and deposited a blanket of glacial material, masking recent structures at the seabed. This complicates the interpretation of recent tectonic activity and the assessment of the risk posed by various faults in the region. However, earthquakes with magnitudes of up to about 4 for have been reported (Weaver and Smith 1983) for major fault zones such as the Devils Mountain, Southern Whidbey Island and Hood Canal - Discovery Bay indicating their current active status.

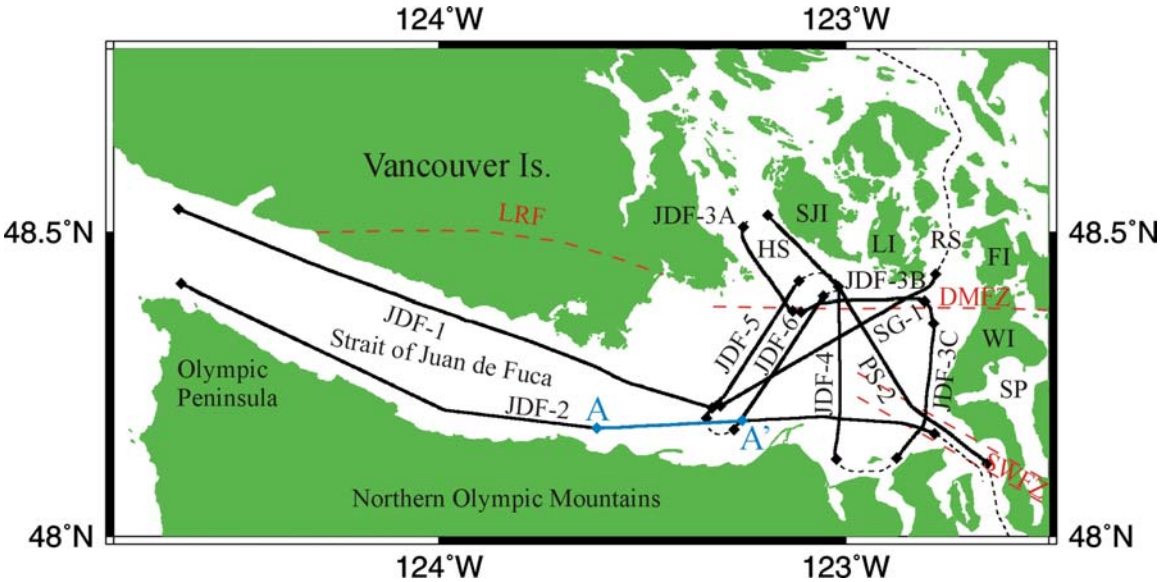

Figure 2. Location of SHIPS seismic lines in the Eastern Strait of Juan de Fuca. Heavy lines = reprocessed seismic data. Heavy blue lines = sections presented in figures 3-6. Fault Zones (schematic): LRF = Long Range, DMFZ = Devils Mountain, SWFZ = Southern Whidbey Island. Straits: HS = Haro, RS = Rosario. Islands: SJI= San Juan, LI= Lopez, FI= Fidalgo, WI= Whidbey.

In this study, seismic reflection data from the Seismic Hazards Investigation in Puget Sound (SHIPS) survey (Fisher et al. 1999) are used to create tomographic velocity models which aid in the geological interpretation of the shallow structure of the Eastern SJDF, providing new information on the region's character and style of deformation.

2. Data Acquisition and Preliminary Processing

Multichannel seismic reflection (MCS) data, acquired in the Seismic Hazards Investigation in Puget Sound (SHIPS) survey (Fisher et al. 1999), were collected using a 16 airgun array (79.3 L) with a shot spacing of 20 seconds. DFS-V instruments recorded 16 seconds of data on a 2.5 km, 96-channel streamer with a 25 m group interval, resulting in a 24 fold data. Initial processing (e.g. Fig. 3) was conducted by the USGS (Fisher et al. 1999). However, as the data were processed to best enhance the general features to 16 s TWTT, they lack clear imaging of the shallow reflections.

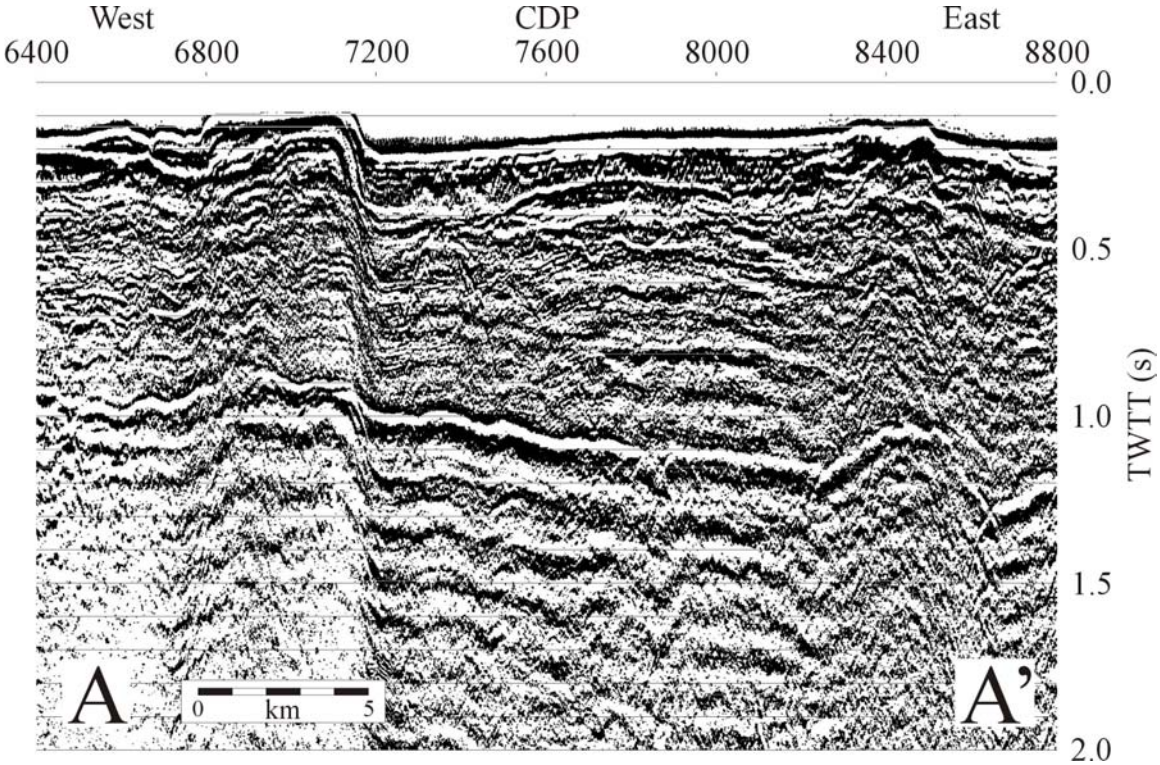

Figure 3. Example section A-A' (Fig. 2 for location) of previously processed seismic reflection data from JDF-2, using constant shot-receiver geometry.

3. New Seismic Reflection Data Processing

Straight-line sections of seismic reflection data from the SHIPS lines JDF-1-6, PS-2 and SG-1 were reprocessed at the Geological Survey of Canada, in order to improve the quality of images in the shallow section (Compare figs. 3 and 4). The geometry was assigned using variable shot spacing, compared with an originally assumed constant shot separation of 50m, allowing for more detailed imaging, especially of the near surface.

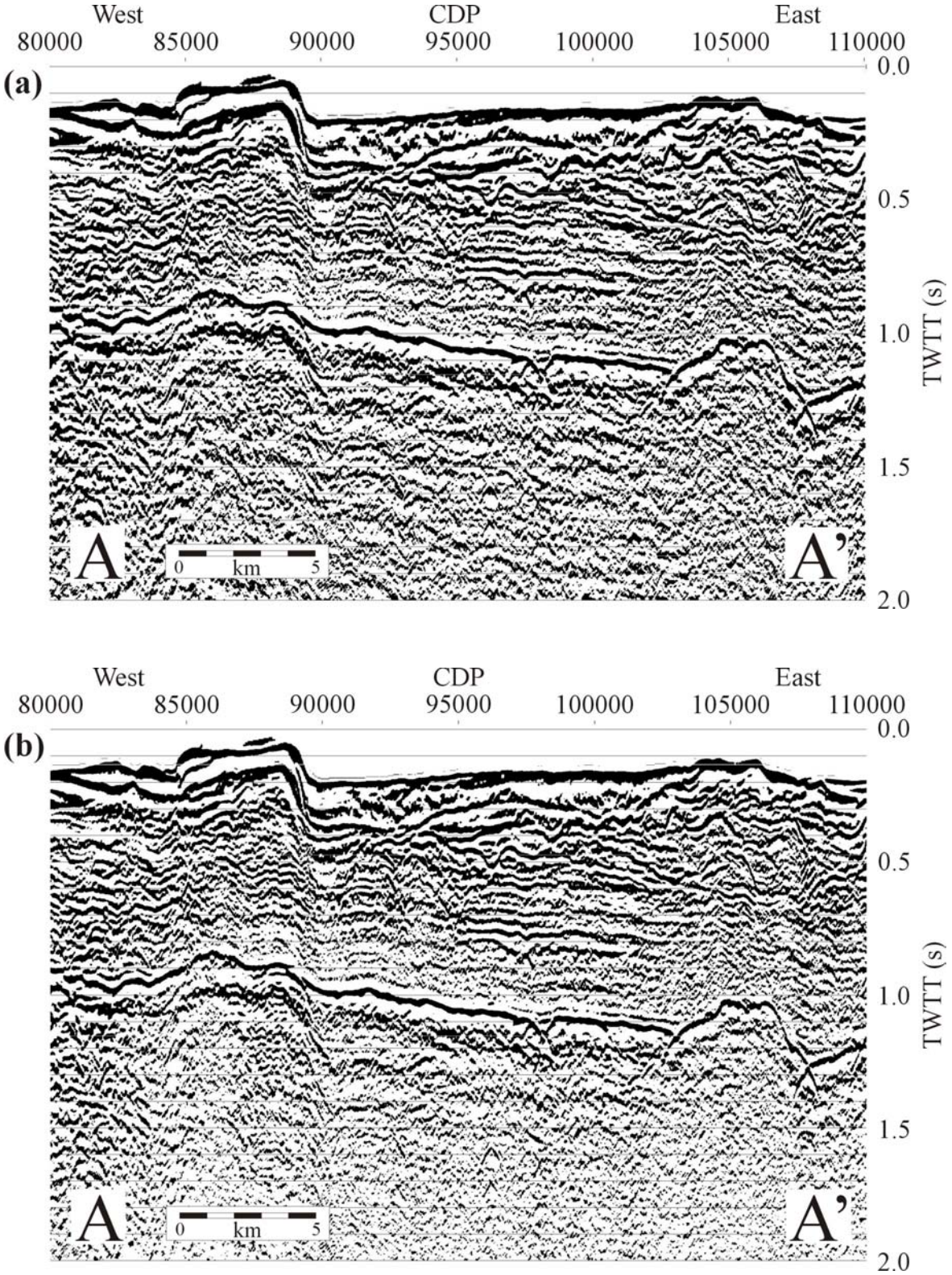

Figure 4. (a) Newly processed section A-A' (Fig. 2) from JDF-2, using variable geometry. **(b)** Example of Tau-P filtering of section shown in figure 4(a).

An amplitude correction was applied for geometrical spreading and the data were deconvolved with a minimum-phase, spiking deconvolution. A surface-consistent amplitude correction was applied and the data filtered with a 57-59--61-63 Hz. notch and 1-6--100-120 Hz. bandpass filter. Software was written to build receiver co-ordinates into the trace headers. Crooked line geometry was then assigned based on a slalom line through the shot/receiver midpoints. This was used to calculate the number and co-ordinates of CDP's in each line segment, which was then used to bin the CDP's. Velocity analysis and NMO were applied prior to slant stacking and rho filtering. Profiles JDF-1-3, PS-2 and SG-1 were also Tau-P filtered in the upper 4 seconds two-way travel-time (TWTT) to suppress multiples.

4. Tomographic Modelling of First Arrivals

First arrival (the direct wave and sub-seafloor refractions) tomographic inversion velocity models (e.g. Fig. 5a), using the true receiver/shot geometry, were calculated for all seismic profiles (Calvert et al. 2000#). An iterative two-dimensional inversion algorithm based on a finite-difference solution to the eikonal equation (Aldridge and Oldenburg, 1993) provides first arrival times to all points of a subsurface velocity grid. Raypaths from each receiver to the source are generated by following the steepest decent direction through the computed travel times. At each iteration a perturbation in the velocity model is calculated from the difference between the calculated and observed first arrival travel times. The velocity of the water layer was set to 1488 ms^{-1} and the seafloor depth estimated from the near-offset reflection data, picked in ProMAX. A 1-D three-layer starting model was estimated from a few trial inversions, followed by 21 iterations using a velocity grid spacing of 25 m.

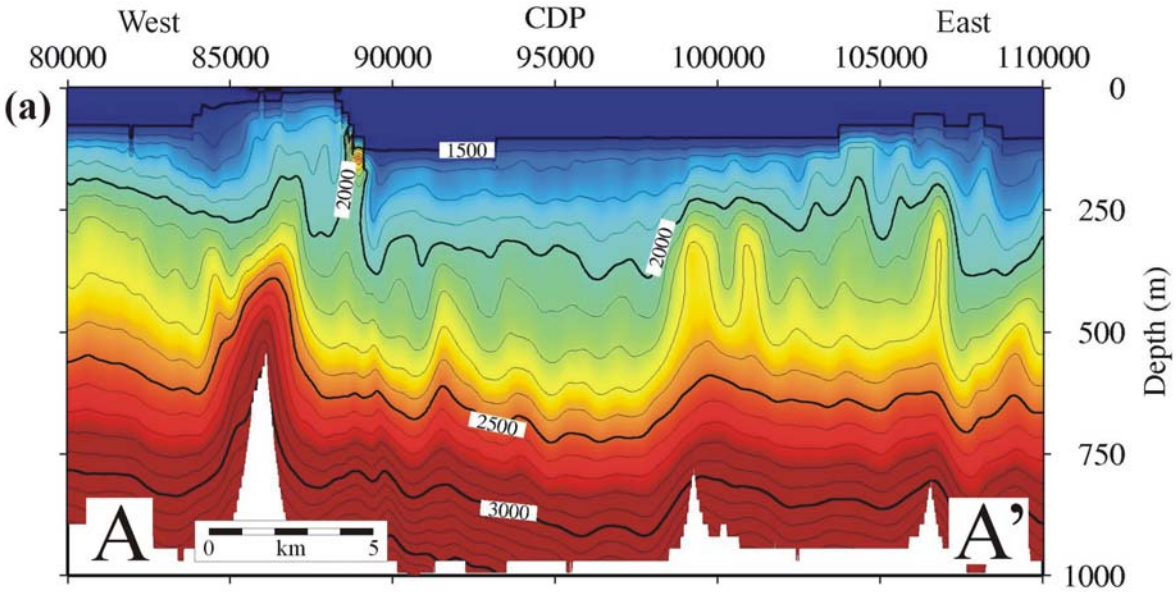

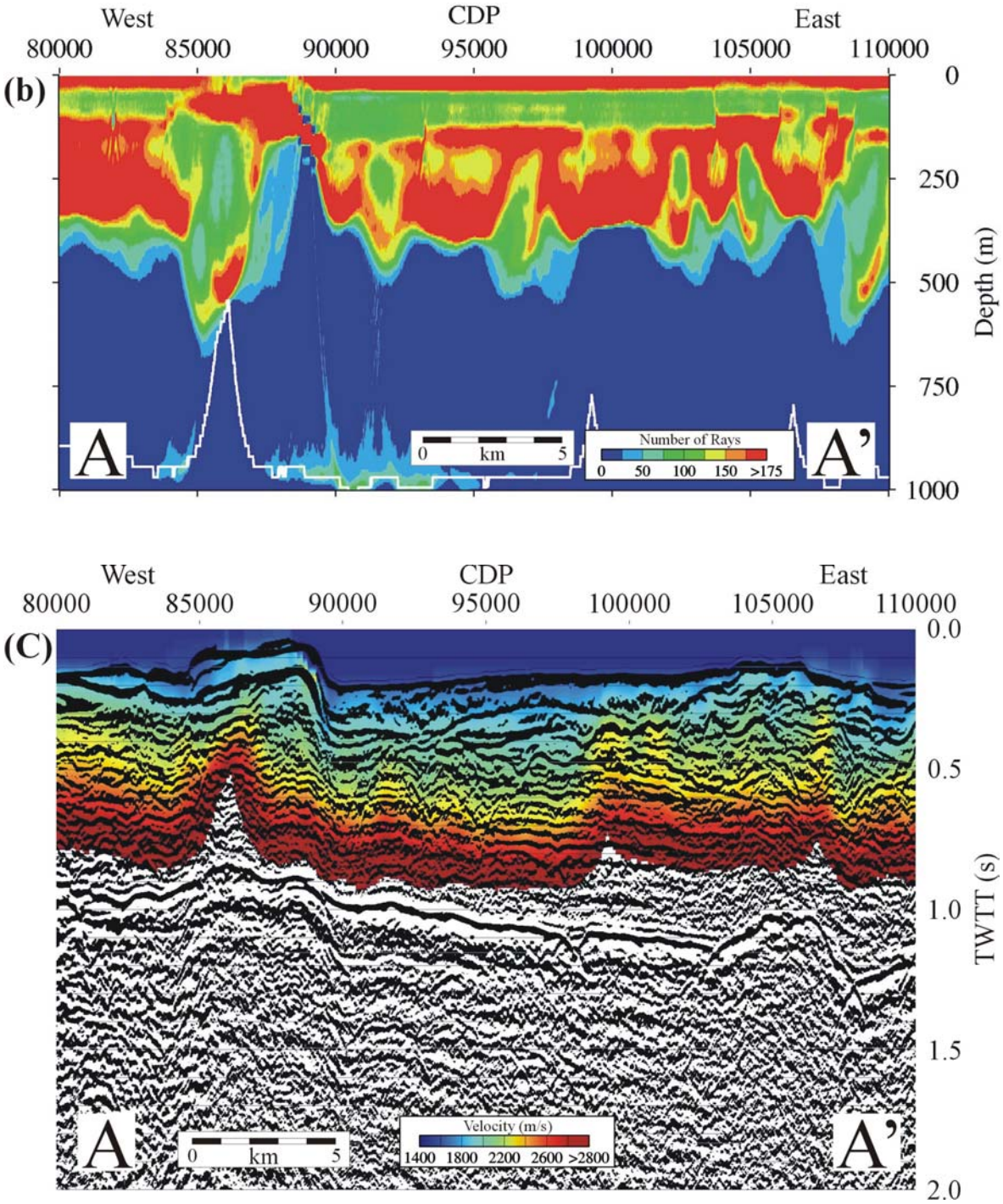

Figure 5. (a) First arrival tomographic velocity model for section A-A' in depth. **(b)** Ray density for model A-A'. Heavy white line shows maximum depth of ray penetration. **(c)** Velocity model (Fig. 5a) converted to TWTT and combined with seismic section A-A' (JDF-2; Fig. 4).

With far offsets of approximately 2600 m and a high density of subsurface raypaths, a high-resolution estimate of P-wave velocity structure is calculated for depths of about 500-1200 m. In the Eastern SJDF velocity models image to a depth greater than the base of the uppermost Pliocene (UPL) in all but the deepest regions of the basin. Plots of ray density (e.g. Fig. 5b) were used to assess the reliability of velocity anomalies.

To facilitate direct comparison of velocity models with seismic profiles, velocity models in depth were converted to two-way travel-time using ProMAX. The velocity models show an overall strong correlation to reflection images (e.g. Fig. 5c), with variation in the magnitudes and gradients of velocity that are concurrent with deformation and changes in stratigraphy.

Calculation of the first horizontal derivative (gradient) is very affective at locating large changes in velocity (Fig. 6), which may occur across steeply dipping faults zones, and were a useful interpretive tool. However, the horizontal gradient models, as with the velocity models, are unreliable in regions of low ray density.

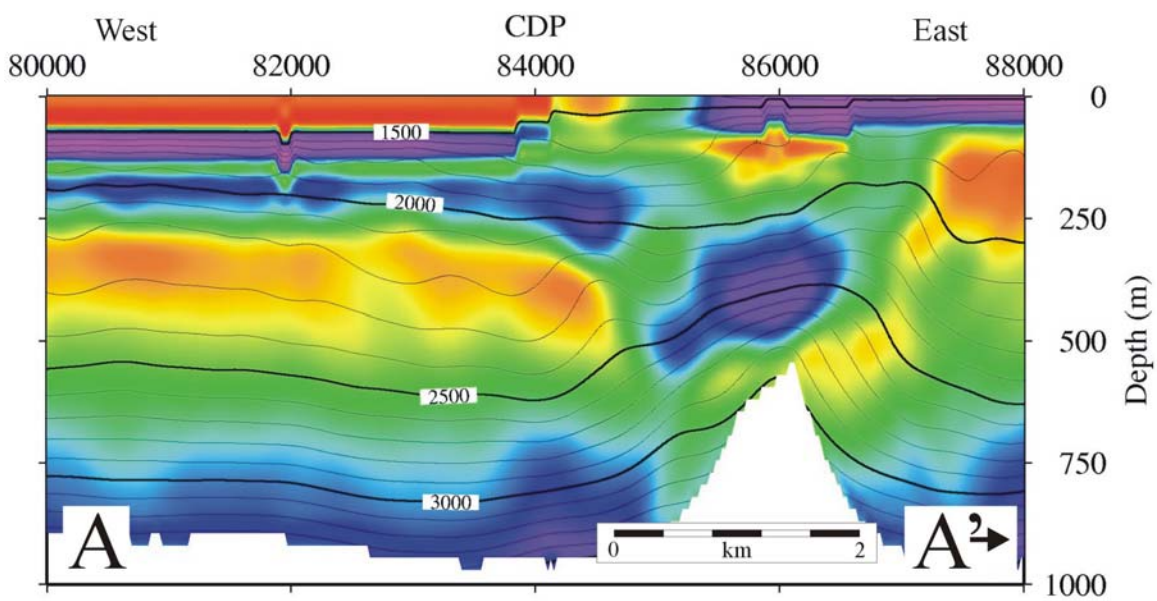

Figure 6. Horizontal gradient model of part of section A-A' illustrating how gradients can clearly indicate the presence of sharp velocity discontinuities which may be associated with steeply dipping faults.

5. Combined Interpretation of Seismic Reflection Profiles and Velocity Models

Interpretations of seismic reflection profiles in combination with tomographic velocity models provide new information on previously identified (e.g. Johnson et al. 2001; Johnson et al. 2000) structures (Fig. 7a). Understanding of their location and style has been enhanced in many areas and several additional features, missed in the interpretation of seismic reflection profiles alone, have been identified.

On a regional scale, structures in the Eastern SJDF follow fairly well defined trends, creating a pattern which has been tied to strike-slip faulting mechanisms (Christie-Blick and Biddle 1985). To the north, the Devil's Mountain fault (DMF) is a fairly discrete east-west trending left-lateral transpressive fault, adjacent to numerous obliquely oriented faults and folds (Fig. 7a), forming a fault zone with a width of greater than 10 km. To the southeast the WNW-ESE trending Southern Whidbey Island Fault (SWF) zone has been interpreted as right-lateral transpressive fault zone, which is composed to three primary faults. To the south and west are numerous faults with a similar trend to the Hood Canal - Discovery Bay fault (HCDBF) zone. Although the majority of structures are clearly associated with these fault zones, in closer detail, deformation is extensive, with numerous structures of varying scale and orientation throughout the region. Johnson et al. (2001) identified a prominent reflection, which marks a major disconformity or unconformity in the region and is suspected to represent the base of the uppermost Pliocene. Here we refer to this datum as the UPL horizon.

5.1. The Devils Mountain, Utsalady Point and Strawberry Point Fault Zones

5.1.1 The Devils Mountain Fault Zone

The Devils Mountain fault (DMF) zone has been identified as one of the major structures in the eastern SJDF and forms the northern boundary of the Everett basin (Johnson et al. 1996). The fault trace has been mapped (Fig. 7) using primarily high resolution and industry seismic reflection profiles (Johnson et al. 2000) from just southeast of Vancouver Island. It may be related to the Long Range fault (MacLeod et al. 1977; Brocher et al. 2001) onshore, which divides the Pre-Tertiary Pacific Rim terrane from the Eocene Crescent terrane. Movement on the DMF may also be taken up by en-echelon structures in Haro Strait (Johnson et al. 2001). The DMF follows an easterly trend across the northeastern SJDF (Johnson et al. 2000), crossing northern Whidbey Island and the Skagit River Delta before turning to the southeast (Oldow 2000) where it merges with the SSE trending Darrington fault (Johnson et al. 1999).

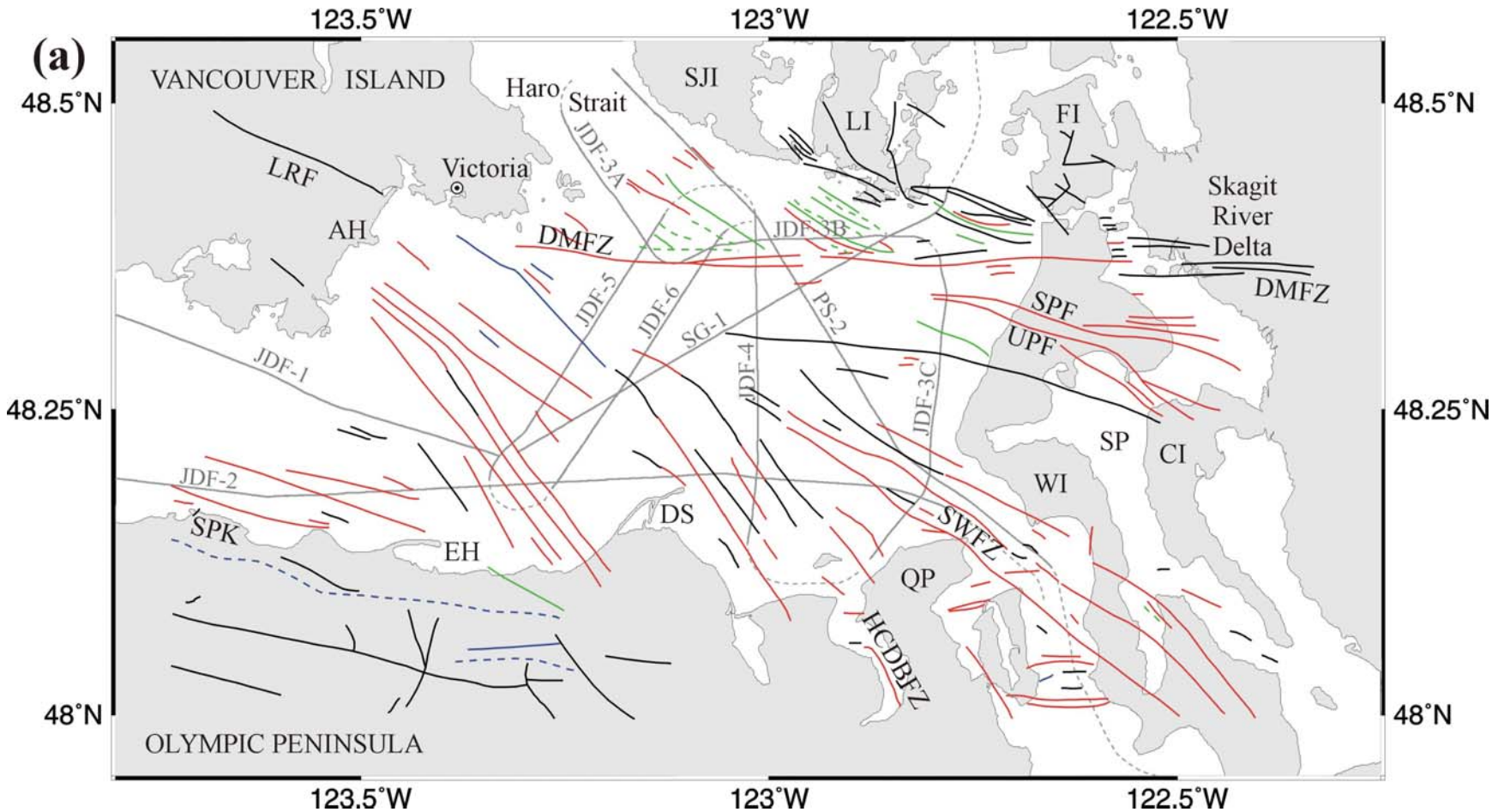

Figure 7(a). Preliminary map of the Tertiary and Quaternary Structures of the Eastern Strait of Juan de Fuca after Johnson et al. (2000). Quaternary Structures: Red lines = faults. Green solid/dashed lines = anticlines/synclines. Pre-Quaternary/Tertiary structures: Black lines = faults. Blue solid/dashed lines = anticlines/synclines. Grey solid/dash lines show the SHIPS survey. Faults/zones: DMFZ = Devils Mountain, SWFZ = Southern Whidbey Island, HCDBFZ = Hood Canal - Discovery Bay, SPF = Strawberry Point, UPF = Utsalady Point, LRF = Long Range. Locations: AH = Albert Head, SPK = Striped Peak, EH = Ediz Hook, DS = Dungeness Spit, QP = Quimper Peninsula, SP = Saratoga Passage. Islands: SJI = San Juan, LI = Lopez, FI = Fidalgo, WI = Whidbey, CI

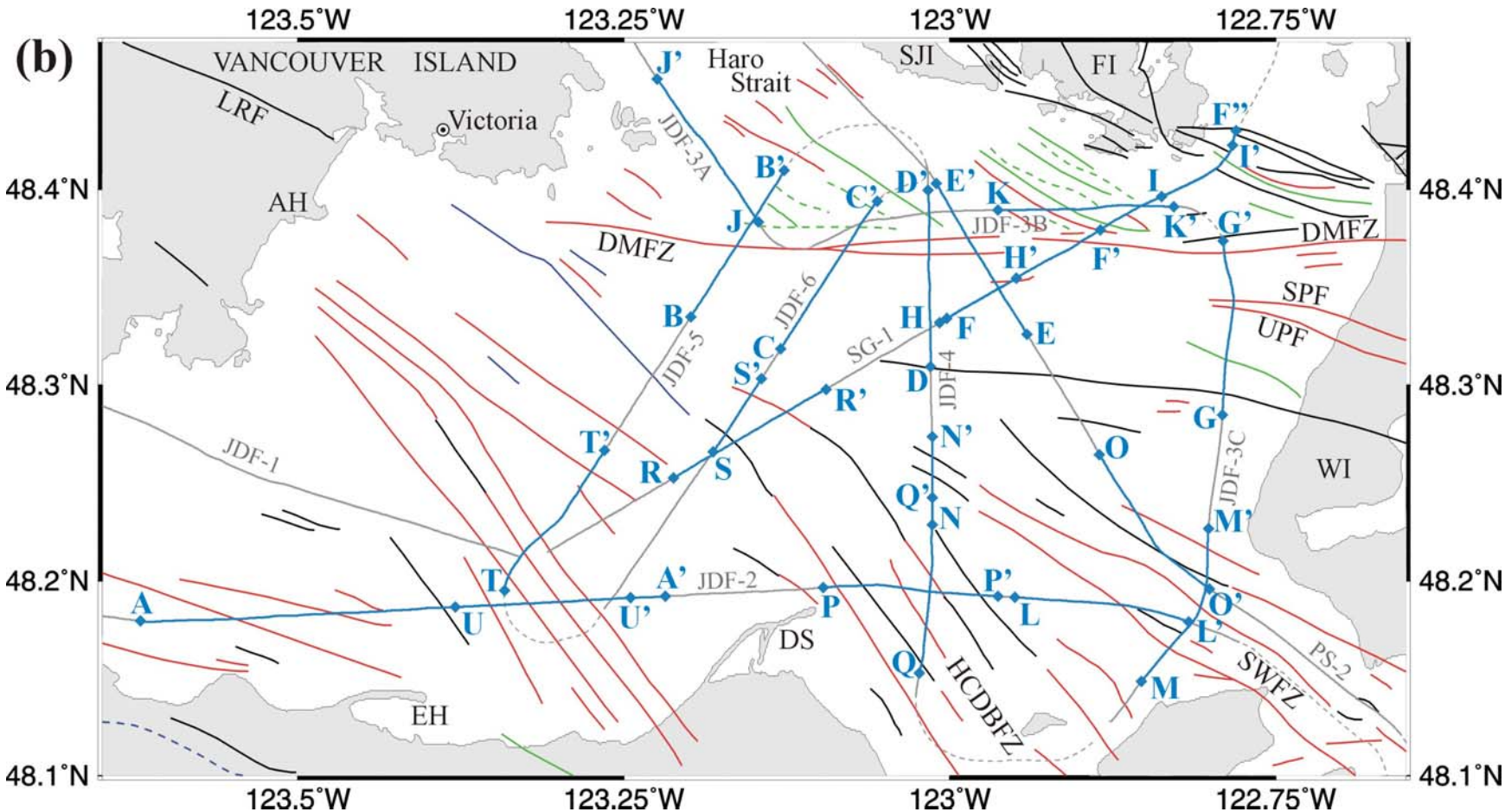

Figure 7(b). Location of seismic reflection sections presented in this report, overlain on structures interpreted by Johnson et al. (2000). Quaternary Structures: Red lines = faults. Green solid/dashed lines = anticlines/synclines. Pre-Quaternary/Tertiary structures: Black lines = faults. Blue solid/dashed lines = anticlines/synclines. Grey solid/dash lines show the SHIPS survey. Faults/zones: DMFZ = Devils Mountain, SWFZ = Southern Whidbey Island, HCDBFZ = Hood Canal - Discovery Bay, SPF = Strawberry Point, UPF = Utsalady Point, LRF = Long Range. Locations: AH = Albert Head, EH = Ediz Hook, DS = Dungeness Spit. Islands: SJI = San Juan, FI = Fidalgo, WI = Whidbey.

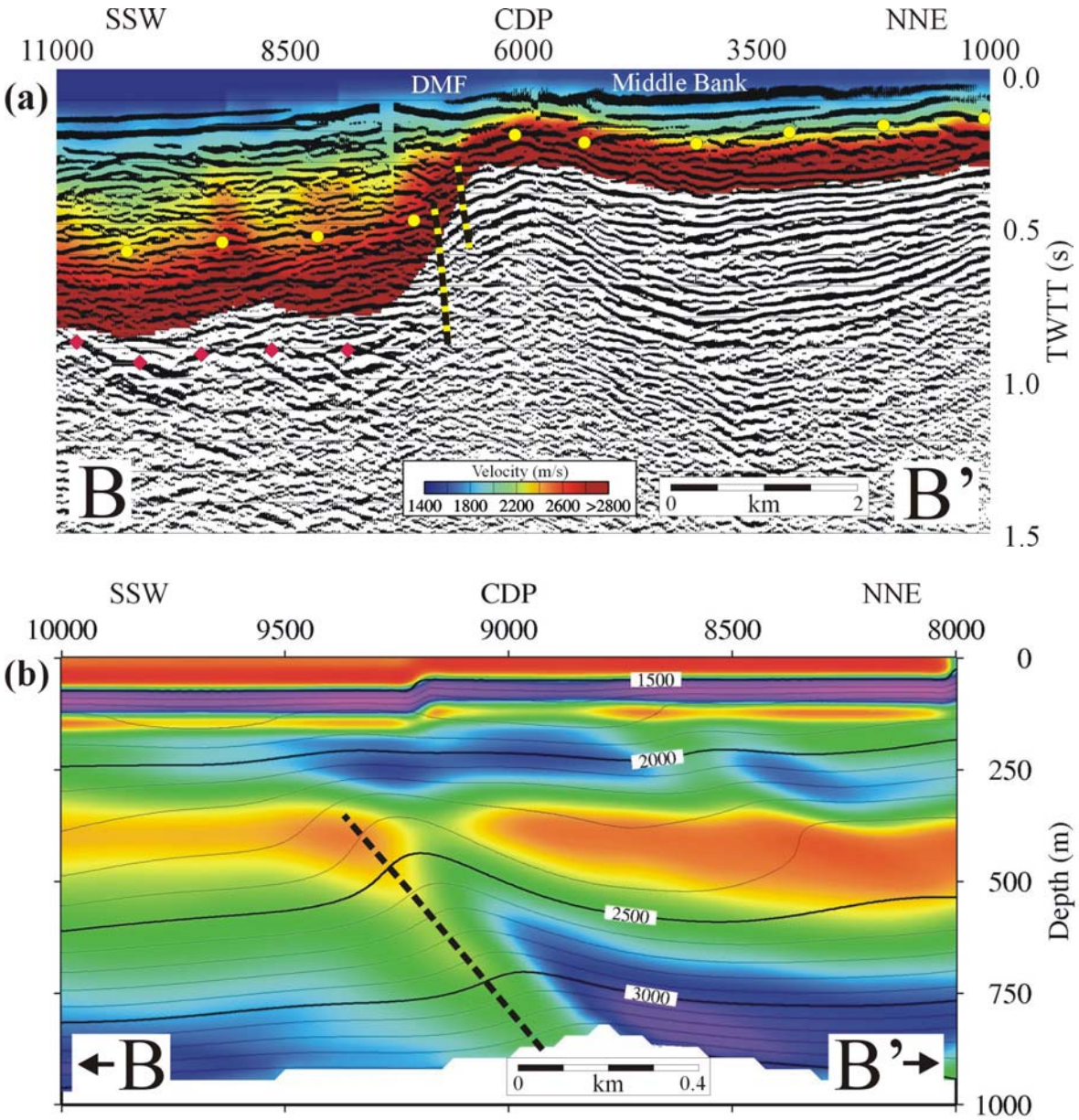

Figure 8 (a) Section B-B' from seismic reflection profile JDF-5, showing the Devils Mountain Fault (Yellow/black dash line). Yellow dots = UPL. Red diamonds = Pre-Tertiary basement. **(b)** Horizontal gradient of a feature to the south of the DMF on JDF-5 (hot colours = high gradient). Contours show velocity (interval = 100 m/s).

The DMF has been interpreted (Johnson et al. 2001) to be a northward dipping (45-75°) left-lateral transpressional master fault, that has been active from the Mesozoic to Quaternary, and associated with numerous WNW trending Quaternary en-echelon structures (Fig. 7).

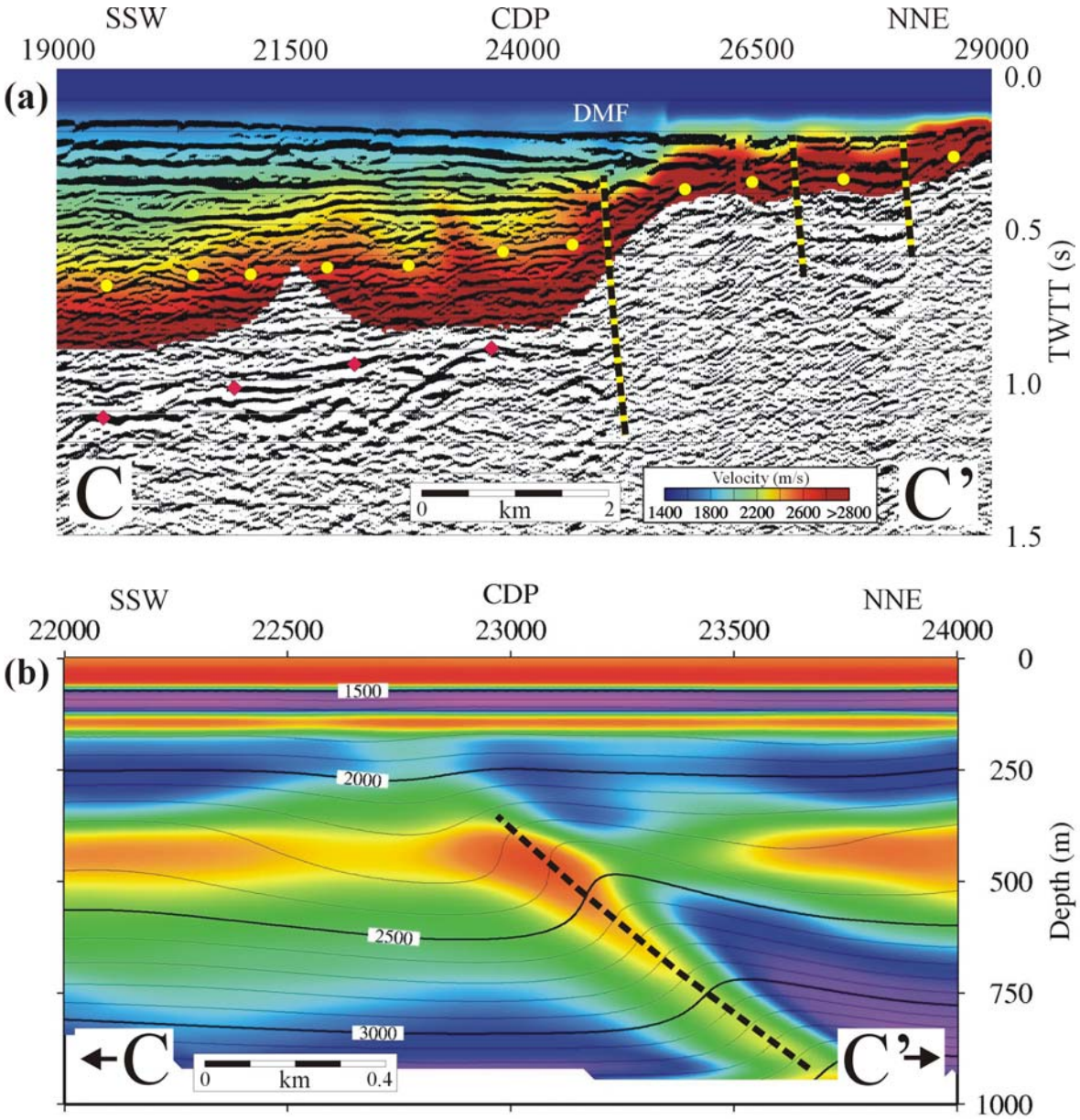

Figure 9 (a) Section C-C' from seismic reflection profile JDF-6 (Fig 7) of the Devil's Mountain Fault (DMF). Yellow dots = UPL. Red diamonds = Pre-Tertiary basement. **(b)** Horizontal gradient of the feature to the south of the DMF zone on JDF-6 (hot colours = high gradient). Contours show velocity (interval 100 m/s).

SHIPS Seismic reflection profiles and new velocity models provide additional information as to the structure and style of the DMF zone and it's along strike variation. The identification of primary structures and the identification of key units, such as the UPL and Pre-Tertiary basement, were in part interpolated from the interpretations of Johnson et al. (2001) and Johnson et al. (2000).

In the northwestern SJDF, seismic profiles JDF-5 and 6 (Figs. 8a and 9a), show the DMF to be associated with a large vertical offset, whose location agrees well with that mapped (Fig. 7) by Johnson et al. (2000). Profile B-B' (JDF-5; Fig 8a) shows a large vertical throw (north side up) of approximately 0.2-0.3 s TWTT for the UPL. This is concurrent with a large offset in velocity model contours of approximately 300 m. The vertical offset of the pre-Tertiary basement exceeds the depth of the velocity models, but seismic profiles suggest it may be greater than 0.4 s TWTT. We interpret the fault to dip steeply to the north with anticlinal folding, characteristic of thrust faulting, of pre-Quaternary rocks in the hanging wall (Fig. 8a).

Profile C-C' (JDF-6; Fig. 9a) shows a somewhat similar structure to JDF-5 across the DMF with a UPL vertical offset of approximately 0.2-0.3 s TWTT. The high velocity gradients to the north of the DMF correspond to the shallow depth (Approximately 0.2-025 s TWTT below seafloor) of the high velocity pre-Tertiary basement, probably of the Wrangellia Terrane (Hyndman et al. 1990), which may underlie the western section of the DMF zone. Profile JDF-6 images deformed Quaternary rocks north of the DMF, interpreted to be folded (Johnson et al. 2000). However velocity models show clear gradients in velocity which cut the shallow sediments and we interpret these to represent faults which disrupt seismic reflections at 0.03 s TWTT and divide the pre-Tertiary basement north of the DMF zone in to 3 fault bound basement blocks (Fig. 9a).

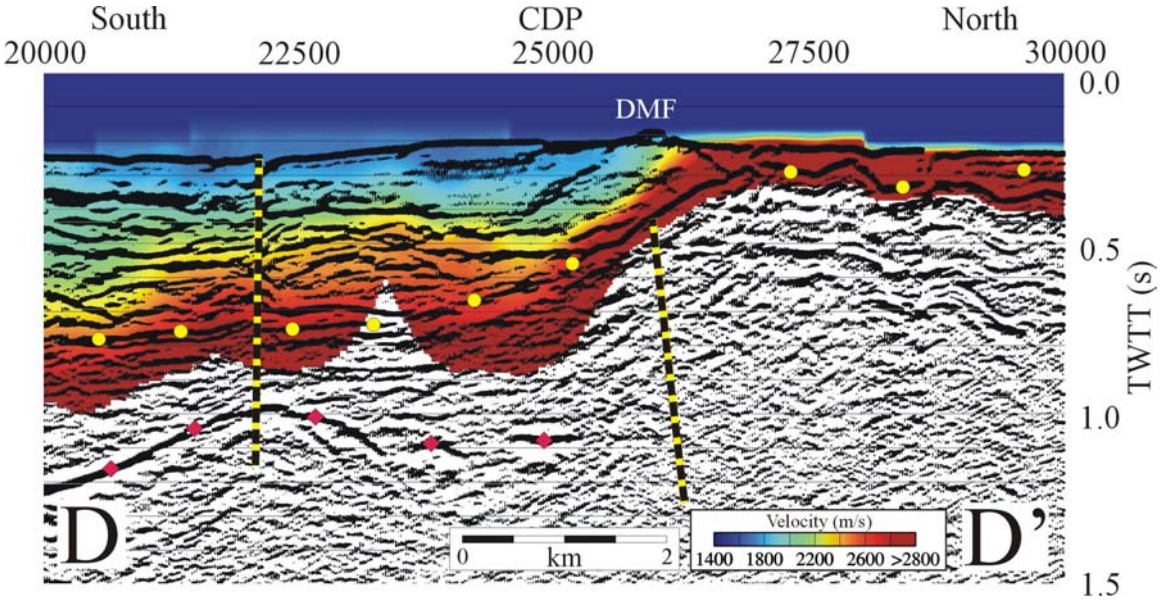

Figure 10. Section D-D' from seismic reflection profile JDF-4 showing the main scarp of the DMF zone. Yellow dots = UPL. Red diamonds = Pre-Tertiary basement.

Seismic section D-D' (JDF-4; Fig. 10), approximately five kilometres to the east, also shows a large step in seismic reflections and velocity contours across a large fault scarp associated with the DMF. The fault has a similar character to observed on profiles JDF-5 and 6 (Figs. 8a and 9a) with a steeply north dipping (45-55° (Johnson et al. 2001))

transpressional fault. The pre-Tertiary basement is offset (up to north) by approximately 0.5 s TWTT, greater than to the east and in part related to the large thickness of post Quaternary rocks (approximately 0.8 s TWTT or about 400 m from velocity models) to the south. The UPL commonly exceeds the depth of the velocity models to the south of the DMF on JDF-4.

Johnson et al. (2000) show the western segment of the fault zone to divide in to two branches at approximately 123.1 W (Fig. 7), based on interpretations (Johnson et al. 2001) of seismic reflection profiles. Section D-D' does show Quaternary faulting to the north of the main fault scarp, but it's vertical offset is relatively minor, suggesting that as with section C-C' (JDF-6) there is substantial fracturing of the pre-Tertiary basement north of the DMF.

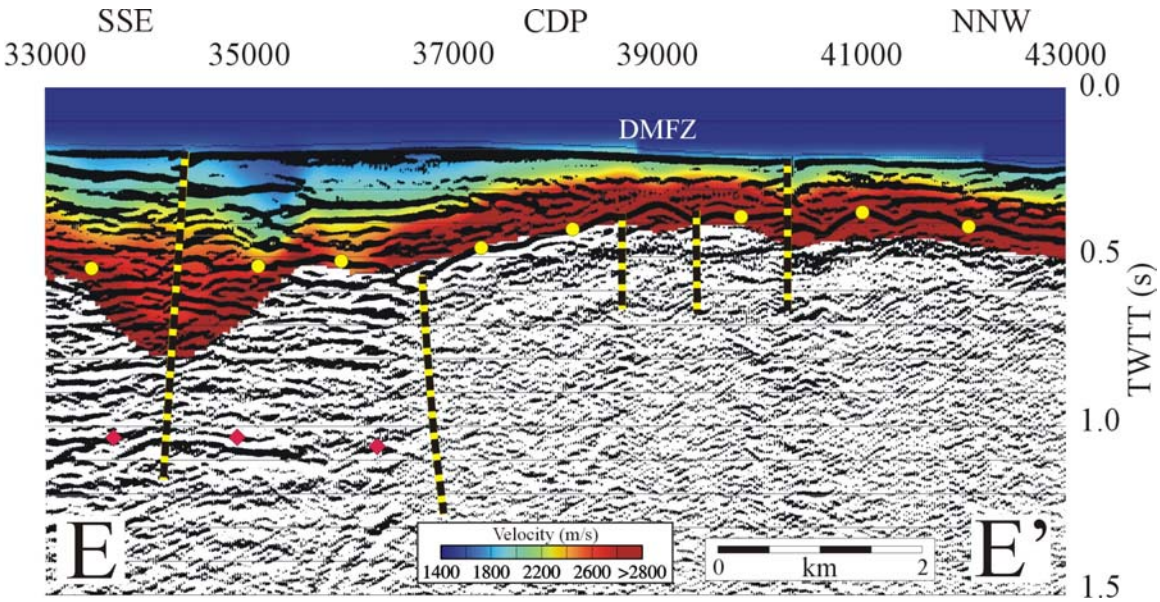

Figure 11. Section E-E' from seismic reflection profile PS-2 showing the primary fault scarp associated with the DMF zone and deformation to the north corresponding to the location of Quaternary deformation in the fault zone. Yellow dots = UPL. Red diamonds = Pre-tertiary basement.

East of JDF-4 (D-D'; Fig. 10) the DMF has been traced (Fig. 7) to continue with an easterly trend (Johnson et al. 2000). Seismic section E-E' (PS-2; Fig. 11) shows minor folding and faulting north of CDP 38000, roughly corresponding to the mapped (Johnson et al. 2000) easterly extension of the DMF (Fig. 7). The vertical offsets are however small, at approximately 0.05 s TWTT or 30 m from velocity models, for the fault at CDP 40300. The location of the primary fault scarp, which displays similar characteristics to profile JDF-4 (Fig. 10) and other western profiles, is located about 1.5 km south of the mapped DMF. Here the pre-Tertiary basement is offset (up to north) by as much as 0.5 s TWTT. The vertical offset of the UPL is much smaller at approximately 0.15-0.2 s TWTT from the seismic profile or approximately 160 m from velocity models, again indicating less vertical movement on the primary fault scarp during the Quaternary.

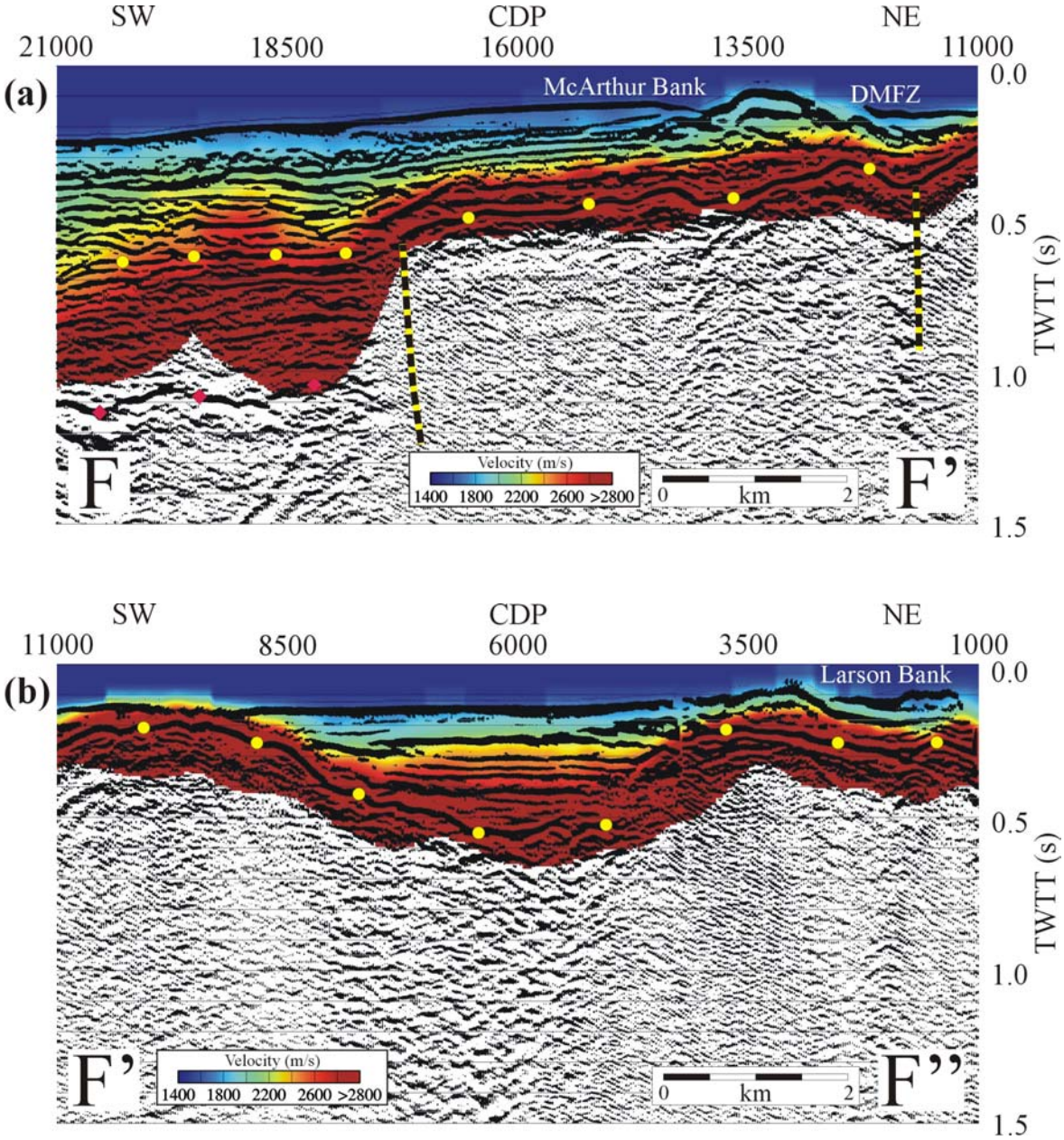

Figure 12. Section F-F'-F" from seismic reflection profile SG-1: **(a)** The DMF zone and primary fault scarp to the south. **(b)** Folding and faulting north of the DMF zone. Yellow dots = UPL. Red diamonds = Pre-Tertiary basement.

Seismic reflection section F-F' (SG-1; Fig. 12a) crosses the mapped DMF zone near CDP 12200, approximately 6 km east of section E-E' (PS-2; Fig. 11), close to McArthur Bank. The fault is not well imaged by profile SG-1, but there are numerous disrupted reflections and subtle fault offsets. A basement uplift between CDP 8000-11000 was interpreted by Johnson et al. 2000 to be bound by two steeply south dipping thrust faults, including the DMF zone. Profile SG-1 (F'-F"; Fig. 12b) shows little evidence for the northerly fault other than the basement relief and we suggest based on reflection terminations (F-F'; Fig. 12a) that the DMF is more likely to be steeply north dipping.

As imaged by section E-E' (PS-2; Fig. 11) the primary fault scarp (CDP 17500) of the DMF zone is located on section F-F' (Fig. 12a) to the south of the mapped DMF. This is very close to the tie between profiles SG-1 and PS-2 (Fig. 7b) making orientation analysis difficult, however we concur with the interpretation (Fig. 7) of Johnson et al. (2000) that it is most likely easterly in orientation. The vertical offset for the UPL is similar to that indicated by other profiles at approximately 0.15 s TWTT or about 160 m estimated from the velocity model. The pre-Tertiary basement shows an offset of a similar magnitude to profile PS-2 of approximately 0.5 s TWTT.

To the east of PS-2, the mapped trace of the DMF zone (Fig. 7) is crossed by JDF-3C (G-G'; Fig. 13). The structure in the region of the DMF zone as mapped by Johnson et al. (2000) is similar to that observed on SG-1. There is a vertical offset, although downthrow to the north, of the pre-Tertiary basement and possibly the UPL of about 0.1 s TWTT, but the overlying Quaternary rocks show smaller offsets. The feature also appears to cut the seabed indicating that there may have been recent activity. The DMF shows only offsets near surface reflections by about 0.05-0.08 s (Velocity model approximately 40-50 m). This indicates that there has been little vertical offset on the DMF this far to the east and agrees with of the Whidbey formation (approximately 80 - 130 Ma - Early Quaternary) fault offsets on Whidbey Island which are only about 4-24 m (Johnson et al. 2001).

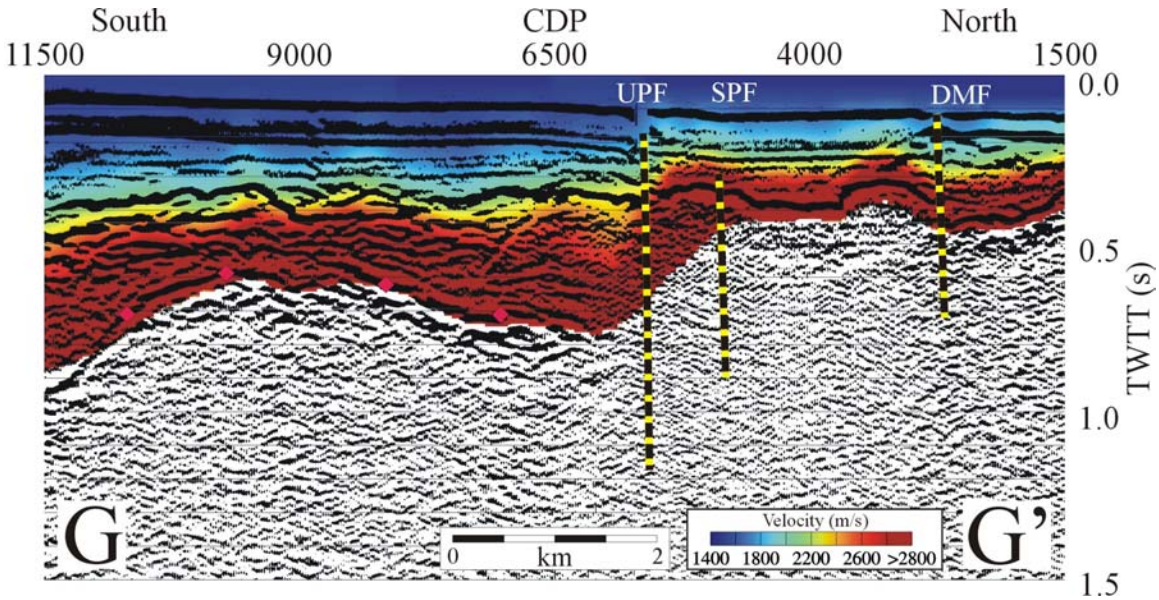

Figure 13. Section G-G' from seismic reflection profile JDF-3C (Fig. 7) across the Strawberry Point (SPF), Utsalady Point (UPF) and Devils Mountain (DMF) faults. Red diamonds = Pre-Tertiary basement.

5.1.2. The Utsalady Point and Strawberry Point Faults

The Utsalady Point fault (UPF) and Strawberry Point fault (SPF) have been mapped (Johnson et al. 2001) to cut the eastern end of the eastern SJDF. Different senses of vertical offset across Whidbey Island (Johnson et al. 2001) suggest that like the DMF, these are left-lateral transpressional faults. The Utsalady Point fault shows the largest vertical offsets (up to north) and forms the southern margin of a pre-Tertiary basement horst (Johnson et al. 2001). Near Whidbey Island Upper Pleistocene strata between the two faults show considerable deformation with dips as high as 45° (Johnson et al. 2001). On section G-G' the UPF has similar characteristics to the large steeply dipping fault scarp of the DMF, interpreted on profiles to the west. Although not clearly imaged, the pre-Tertiary basement may have a vertical throw of about 0.3 s TWTT. Velocity models suggest a throw of about 300 m. The UPL is vertically offset by about 0.02-0.03 s TWTT (approximately 60 m from velocity models), with smaller offsets of overlying rocks, indicating Quaternary motion on this fault. These offsets are much lower than the interpretation of 200-300 m by Johnson et al. (2001) for the UPL, inferred from seismic reflection profiles and well data on Whidbey Island, indicating greater offsets to the east.

The Strawberry Point fault, on section G-G' (JDF-3C; Fig. 13), appears to be a much smaller feature than the Utsalady Point fault, with an up to south sense of throw and a steep dip. The UPL appears to have been vertically offset by about 0.08 s TWTT (40 m from velocity models), with smaller offsets for the overlying Quaternary rocks. Johnson et al. (2001) estimate 80-200 m uplift of the UPL on the west side of Whidbey Island, but only a few meters of offset in the last 1750 years. Perhaps also indicating greater offsets for the SPF, as with the UPF, to the east.

5.1.3. Secondary faulting associated with the Devils Mountain fault zone.

Mapping by Johnson et al. (2000) revealed numerous compressional and transpressional features oblique to the DMF to have a strike-slip association (Christie-Blick and Biddle 1985). Seismic reflection profiles and tomographic velocity models are useful in providing additional information on some of the previously mapped structures and in identifying new ones.

To the south of the DMF, sections B-B' (JDF-5; Fig. 8) and C-C' (JDF-6; Fig. 9) show velocity highs at approximately CDP 9500 and CDP 23500 respectively. Although ray density is low below 400 m, a high density above indicates that the crests of these features are well constrained. Subtly broken reflections below the UPL, suggest a fairly steeply southward dipping thrust or transpressional fault, which exhibits a small (up to north) vertical offset of approximately 0.02 s TWTT. Velocity models suggest an offset of about 50 m and a southward dip of about 40-50 degrees (Figs 8b and 9b). The similarities between the two sections suggest that the feature is continuous between the two profiles and its character suggests that it represents a secondary transpressional fault associated with the DMF, but with little evidence for more recent deformation.

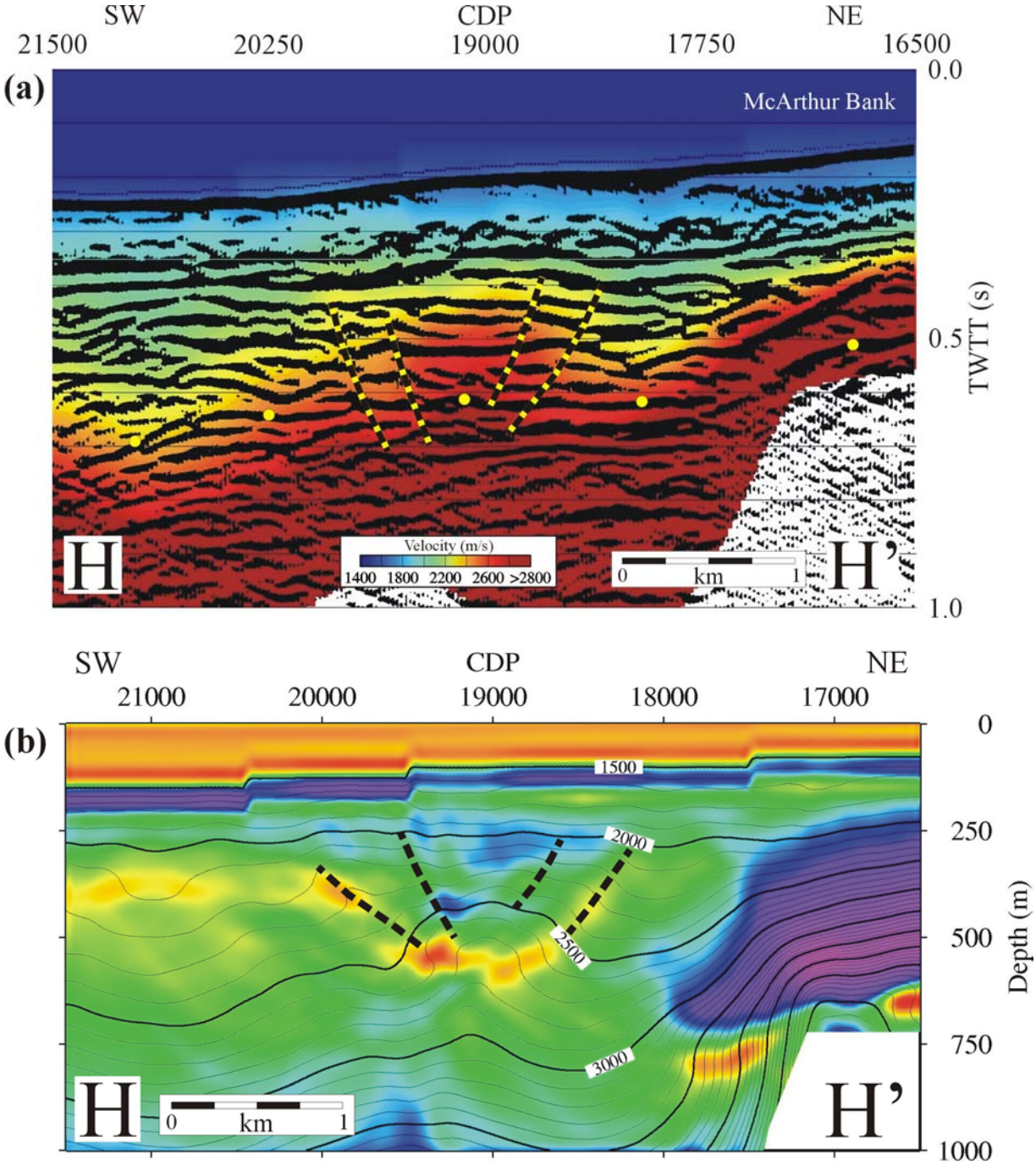

Figure 14. (a) Seismic reflection section from SG-1 showing faulting to the south of the Devils Mountain fault. Yellow dots = UPL. **(b)** Tomographic velocity model from SG-1. Black contours show velocity (interval 100 m/s). Colour bitmap shows the horizontal gradient of velocity. Hot colours = high gradient.

South of the primary fault scarp on section H-H' (SG-1; Fig. 14a) enhancement by velocity models and the horizontal gradient of velocity (Fig. 14b) reveals a velocity high with several radiating near linear velocity anomalies which appear to converge at a depth

of about 700 m. These anomalies correspond to broken reflections on seismic sections that show variable senses of offset and may represent a flower structure. Dips estimated from the velocity model (approximately 30-40 degrees) may be biased by the raypaths.

Several other faults and folds on profile SG-1 are probably associated with the DMF. A decrease in the magnitude and vertical gradient of velocity to the south of CDP 4500 (SG-1; Fig. 15) corresponds to pre-Quaternary faulting (Johnson et al. 2000), which we re-interpret to dip northward. At approximately CDP 5500-6000 (Fig. 15) a thrust fault appears to cut Quaternary rocks. To the south of the DMF (CDP 12500-16000) numerous folds in the UPL may be associated with faulting (Fig. 12a).

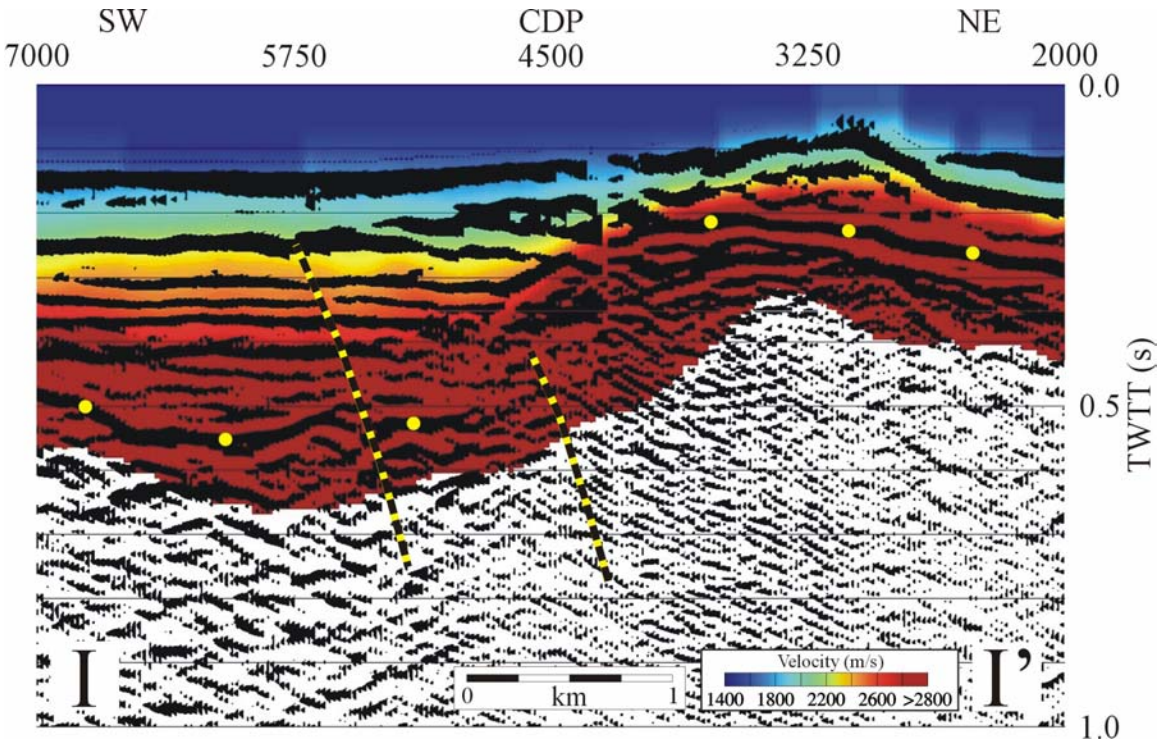

Figure 15. (a) Seismic reflection profile from SG-1 showing thrust faulting north of the DMF. Yellow dots = UPL.

North of the DMF in Haro Strait, section J-J' (JDF-3A; Fig. 16) shows very high velocities and gradients (approximately 12.5-25 m/s/m) associated with the shallow pre-Tertiary (probably Wrangellia) basement. Ray density is good down to 300 m indicating a well-constrained velocity model structure. We interpret a number of faults just to the north of and in addition to Quaternary synclinal folding interpreted by Johnson et al. (2000) at approximately CDP 16000.

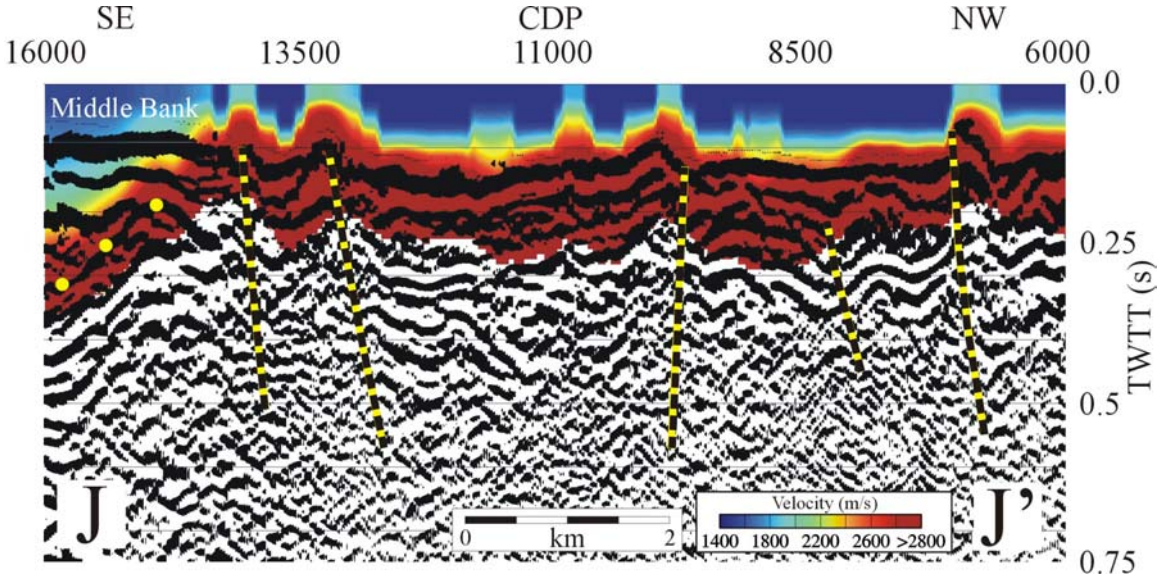

Figure 16. Section J-J' from seismic reflection profile JDF-3A, showing faulting and deformation to the north of the DMF in Haro Strait. Yellow dots = UPL.

Two faults interpreted from velocity models and seismic section J-J' (near CDP 13500; Fig. 16) show steep northward dips and offsets of about 0.02 s TWTT (approximately 20-40 m from velocity model). The faults cut the very shallow surface and indicate Quaternary motion with a component of compression and may represent some of the motion on the DMF that may be taken up by deformation in Haro Strait as suggested by Johnson et al. (2001). Other small offset Quaternary faults are imaged further to the northwest near CDP's 10000, 8000, 7000 and 4000.

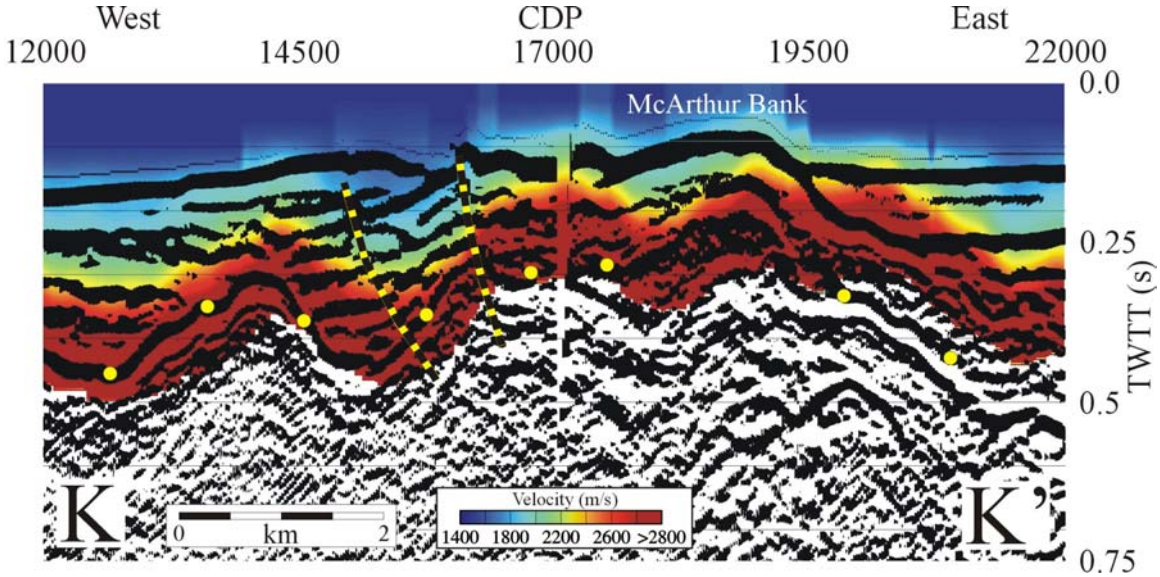

Figure 17. Section K-K' from seismic reflection profile JDF-3B showing folding of the UPL and the differential deformation of more recent Quaternary units. Yellow dots = UPL.

Further east along the Devils Mountain fault zone, section K-K' (JDF-3B; Fig. 17), near parallel to and just north of the DMF (Fig. 7b), images many structures associated with the fault zone. The UPL is strongly deformed, but overlying Quaternary rocks are generally flat lying with discrete zones of deformation, indicating little deformation since the beginning of the Quaternary. Our interpretations broadly agree with those of Johnson et al. (2000), but we have identified additional Quaternary structures. Between approximately CDP 15000 - 20000 (Fig. 17) Quaternary rocks show shallow high angle faulting which accompanies folding. The onlap of more recent flat lying units between CDP 19000-20000 may indicate that this folding and deformation is not recent, however to the west between CDP 13000-15000 more recent deformation has affected these units indicating that more recent deformation occurs in discreet zones.

5.2. The Southern Whidbey Island Fault Zone

The Southern Whidbey Island fault (SWF) zone is a major right-lateral transpressional fault zone in the SJDF (Pratt et al. 1997; Weaver and Smith 1983), antithetic (Christie-Blick and Biddle 1985) to the DMF zone. Previous interpretations (Johnson et al. 2000) have indicated three primary faults with much along strike structural variation.

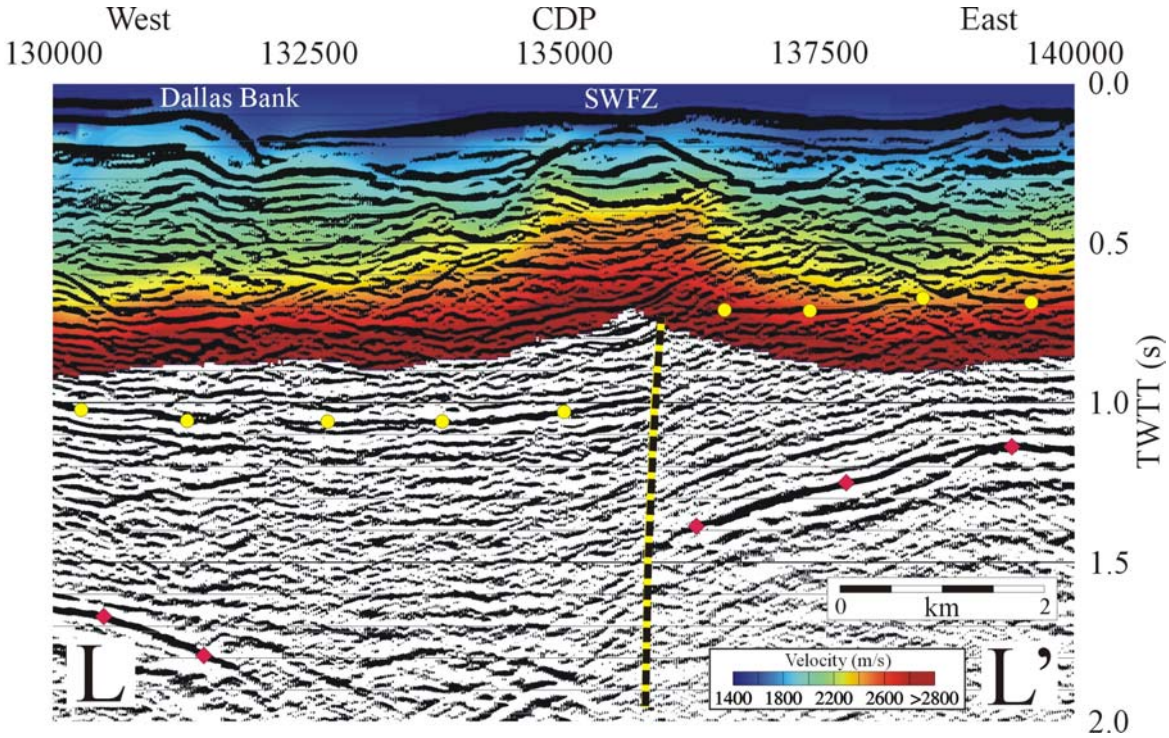

Figure 18. Section L-L' from seismic reflection profile JDF-2, showing the westerly of three strands of the Southern Whidbey Island fault zone (SWFZ). Yellow dots = UPL. Red diamonds = Pre-Tertiary basement.

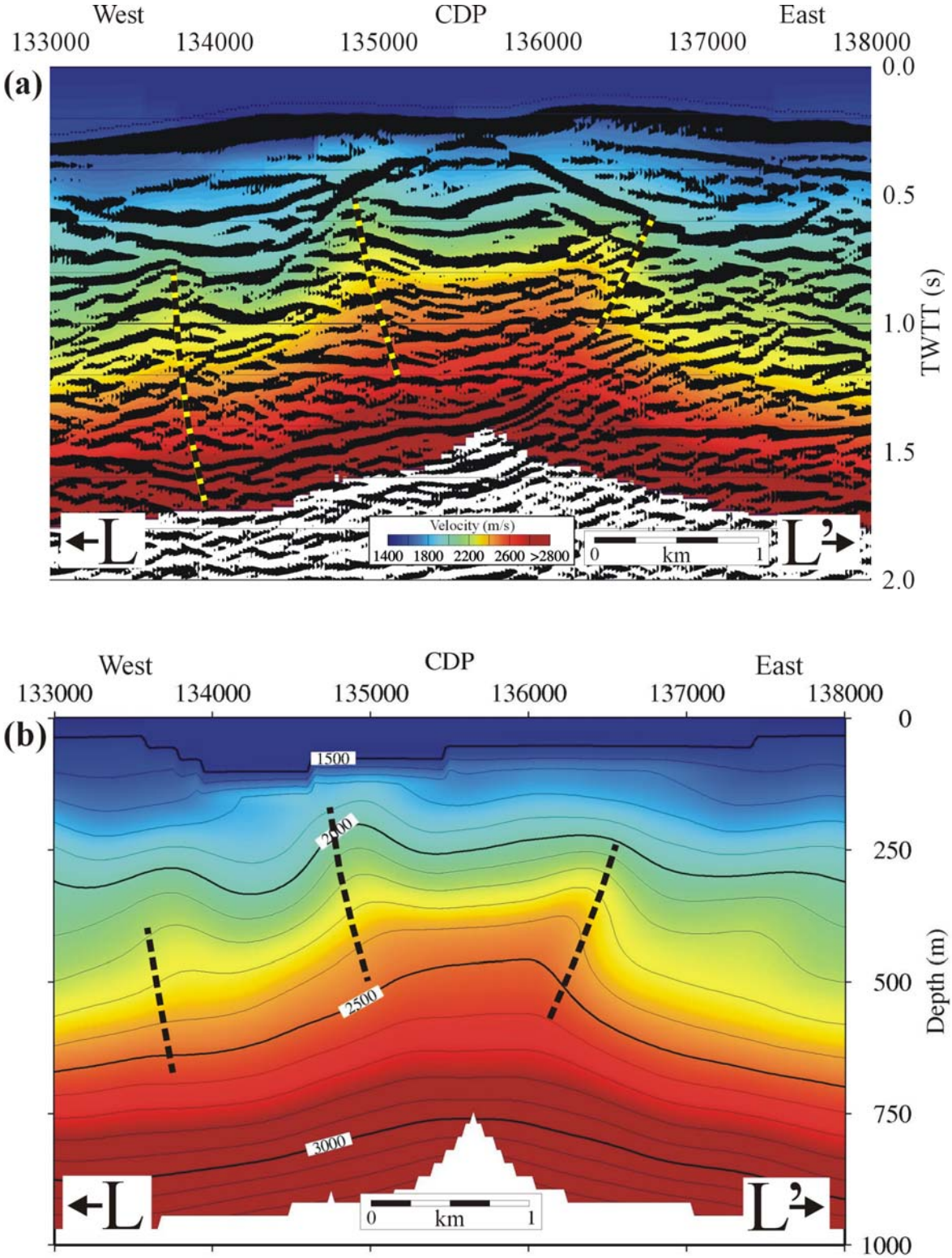

Figure 19. (a) Seismic section from JDF-2, showing the possible flower structure associated with the SWF zone. **(b)** Velocity model. Contour interval 100 m/s.

The SWF zone is imaged by four seismic profiles from the SHIPS survey, and is most clearly imaged by section L-L' (JDF-2; Fig. 18). A steeply dipping fault at CDP 136000 offsets (down to west) the pre-Tertiary basement by approx. 0.5 s TWTT. The basement and thick overlying pre-Quaternary rocks dip (approx. 10-15 degrees) gradually towards the fault from the west and the pre-Tertiary basement just to the east of the fault has been tilted towards the west. The UPL shows a similar, but smaller offset of about 0.27 s TWTT, indicating motion during deposition of Pre-Quaternary units. Faulting and fracturing of units above the UPL and reflection offsets near to the seabed indicate that motion on the fault has continued until recent time.

Seismic profile JDF-2 (Figs. 18 and 19a) and the tomographic velocity model (Fig. 19b) image a pair of inward dipping thrust faults at CDP 134900 and 136600 which bound an uplifted block of Quaternary rocks, which appears to have been affected by subsidiary faulting. The velocity model (Fig. 19b) suggests that the faults dip at 40-60 degrees. The deformation is associated with the major transpressional fault below (Fig. 18) and may represent a flower structure.

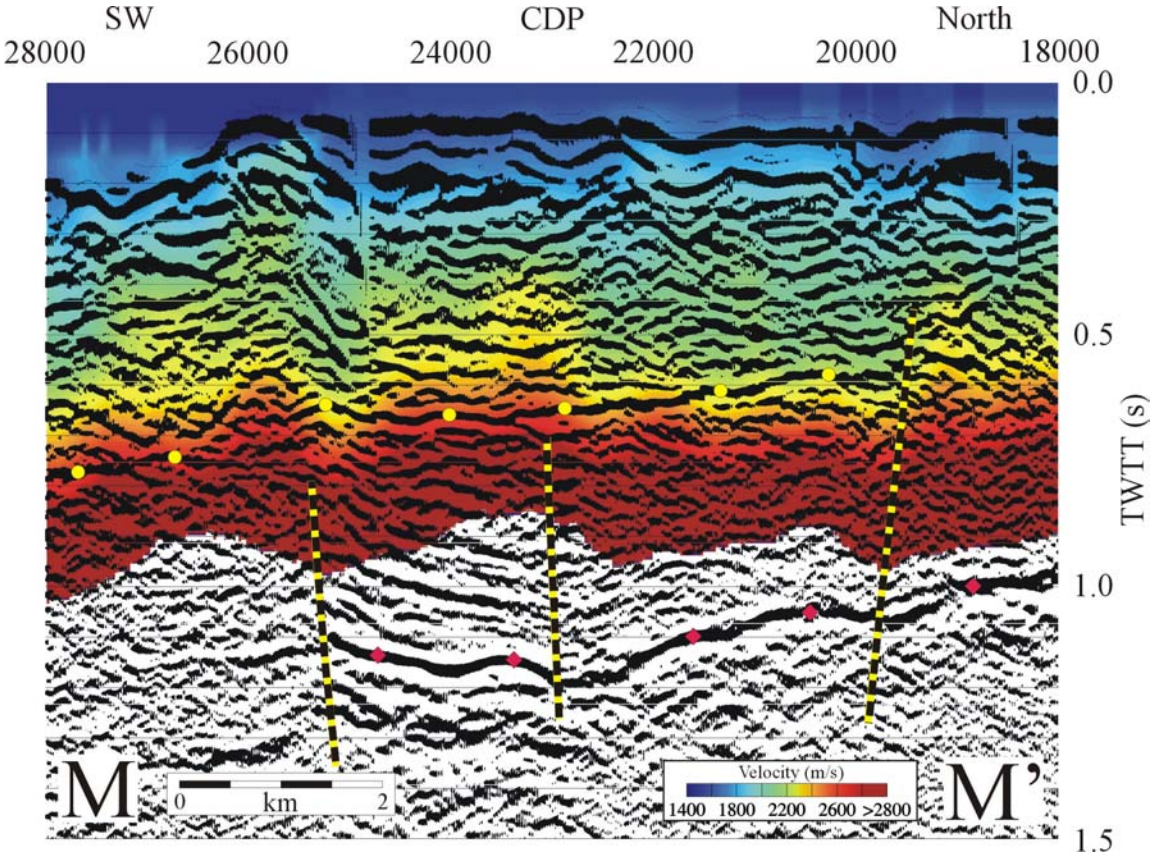

Figure 20. Section M-M' from seismic profile JDF-3C across the entire SWF zone. Yellow dots = UPL. Red diamonds = Pre-Tertiary basement.

Section M-M' (JDF-3C; Fig. 20) gives a cross section of the entire SWF zone including the fault strand imaged by JDF-2 (CDP 25500; Fig. 20/CDP 136000; Fig. 18). The pre-

Tertiary basement across this strand of the SWF zone is not clearly imaged to the south of the fault, but the vertical offset (up to north) of may exceed 0.2 s TWTT. The UPL shows a vertical offset (up to north) of about 0.1 s TWTT, much less than on profile JDF-2, approximately 4 km to the northwest, indicating along strike variation. To the east, in the centre of the SWF zone, the pre-Tertiary basement dips at about 10-20 degrees northwards, different in direction to profile JDF-2. These variations in dip and offset indicate that deformation within the SWF zone is complex and highly variable along strike.

To the north, seismic profile JDF-3C images two other faults associated with the SWF zone. The first at approximately CDP 22500 is indicated by steep horizontal gradients in the velocity models at depths of about 350-450 m, with little much smoother velocities at shallower depths. Reflection offsets associated with this feature appear to be quite small, however reflections both in the Quaternary section and the pre-Tertiary basement show variations in dip on either side of the fault, characteristic of strike-slip faulting. Another velocity anomaly at approximately CDP 19000 is related to another fault strand of the SWF zone. Velocity anomalies are observed to a shallow depth that corresponds to a deflection (up to north) of the UPL of about 0.05 s TWTT and a small depression in the pre-Tertiary basement of a similar magnitude.

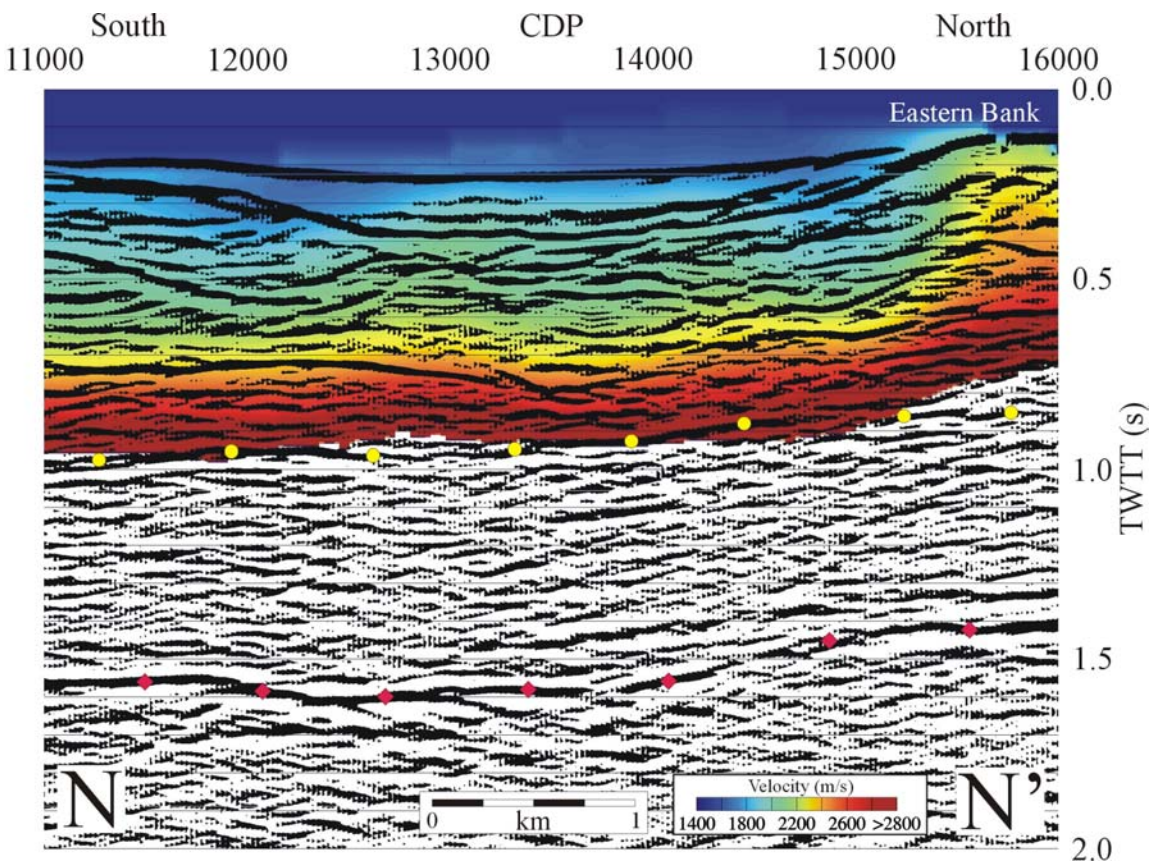

Figure 21. Section N-N' from seismic reflection profile JDF-4 across the SWF zone. Yellow dots = UPL. Red diamonds = Pre-Tertiary basement.

Section N-N' (JDF-4; Fig. 21) images the northwestern end of the SWF zone, where Johnson et al. (2000) have suggested pre-Quaternary motion on two faults at approximately CDP 13900 and 14900. Broken reflections, with minor offsets are observed as shallow as 0.4 s TWTT and may be associated with deflections of about 0.1 s TWTT of the pre-Tertiary basement. Although the features do appear to cut Quaternary rocks above the UPL, they do not appear to affect more recent units shallower than about 0.3 s TWTT, indicating Quaternary, but no recent motion at the westerly end of the SWF zone.

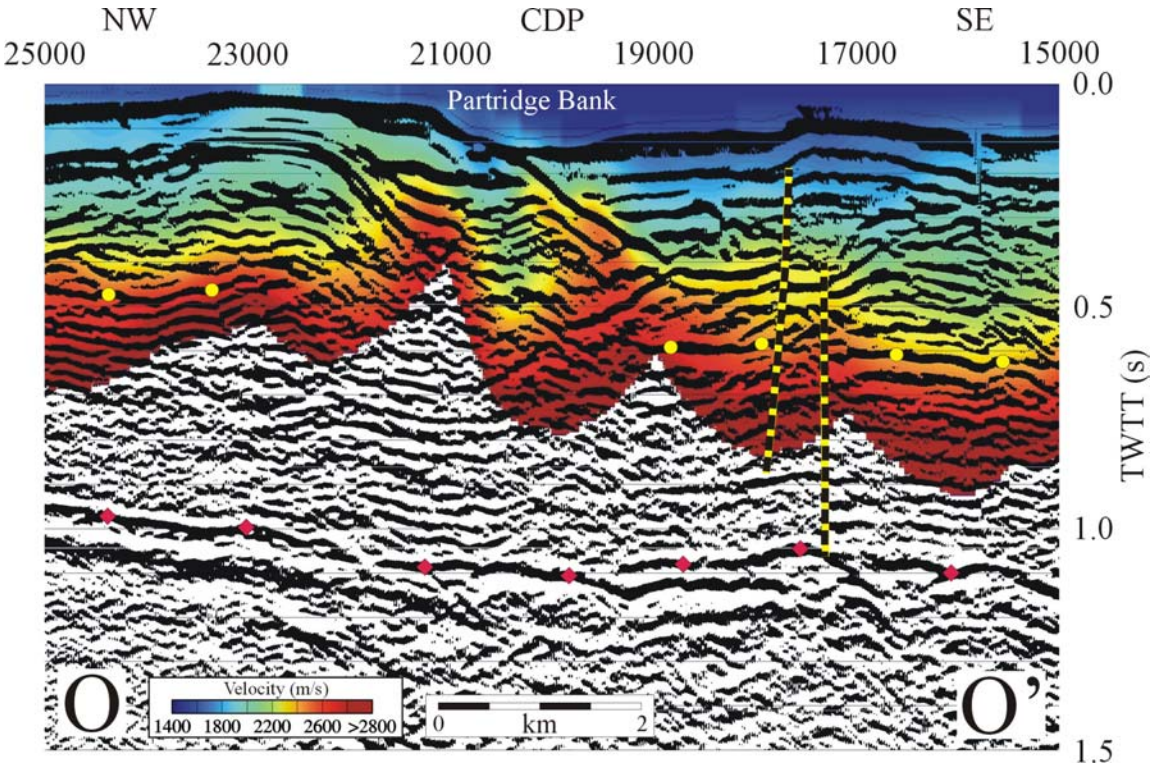

Figure 22. Section O-O' from seismic reflection profile PS-2 across the SWF zone. Yellow dots = UPL. Red diamonds = Pre-Tertiary basement.

Section O-O' (PS-2; Fig. 22) crosses the northern primary strand, as mapped by Johnson et al. (2000), of the SWF zone. At approximately CDP 17700 steeply dipping faulting affects the pre-Tertiary basement and appears to offset the seabed. Reflections show lower dips than to the north and the offsets, which are less than 0.03 s TWTT show variation of the sense of offset with depth, characteristic of strike-slip faulting. Our interpretations indicate that this strand of the SWF zone was active in the Quaternary further west than suggested by Johnson et al. (2000). To the north at approximately CDP 21100 a large velocity anomaly high corresponds to the southeastern edge of Partridge bank and shallow to steeply dipping broken reflections in the Quaternary section, as far southeast as CDP 19000. The pre-Tertiary basement however shows only minor perturbations with a gradual decrease in depth towards the northwest.

5.3. Faults to the south and west of the DMF and SWF zones

Numerous NW-SE trending faults have been interpreted (Johnson et al. 2000) to the south of the DMF zone. Adjacent to Vancouver Island the faults generally trend WNW (approx. N 50° W), but rotate to a NW orientation to the east, perhaps influenced by the structure of the pre-Tertiary basement. Fault orientations, although steeper than deformation associated with the DMF and SWF zones, are consistent with the regional strike-slip domain associated with a Devils Mountain master fault.

5.3.1 Northwestern extension of the Hood Canal- Discovery Bay fault zone.

The Hood Canal - Discovery Bay fault zone follows a topographic low in the eastern Olympic Peninsula, between Discovery Bay and Hood Canal (Roberts 1991) and is related to the eastern edge of the Crescent terrane. Faults related to its extension to the northwest have been imaged by seismic reflection profiles JDF-2, 4 and 6, and SG-1.

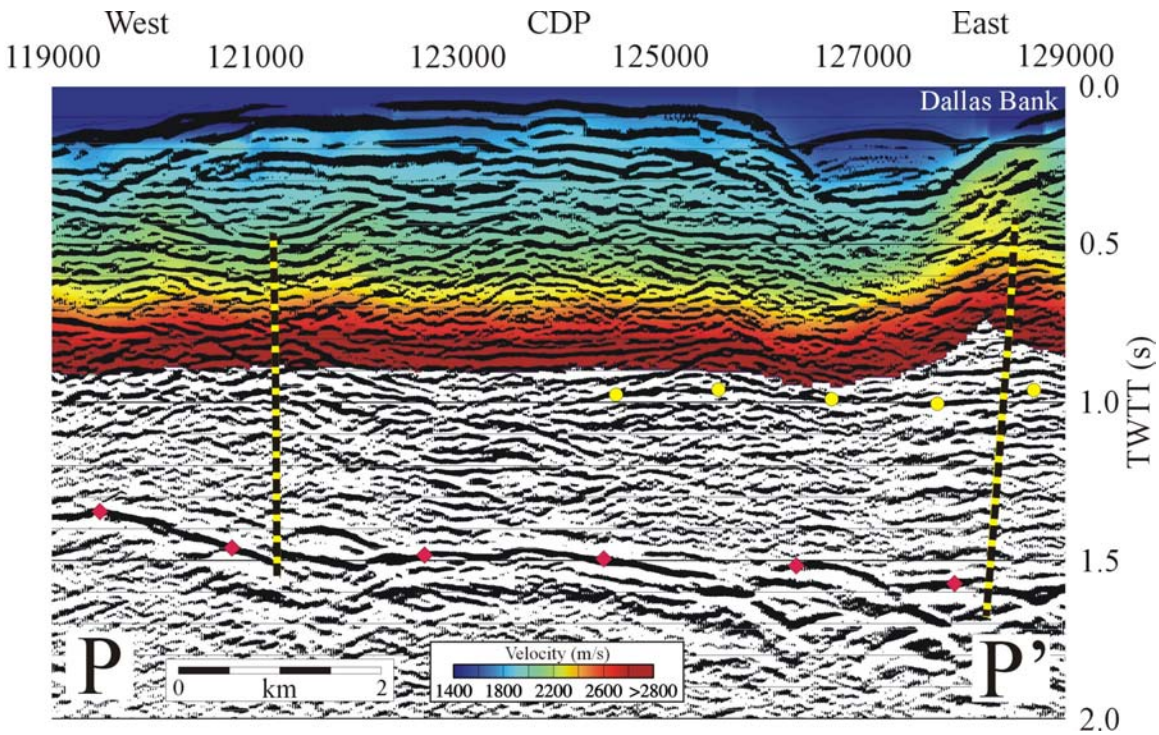

Figure 23. Section P-P' from seismic reflection profile JDF-2 across the NW extension of the Hood Canal -Discovery Bay fault zone. Yellow dots = UPL. Red diamonds = Pre-tertiary basement.

Section P-P' (JDF-2; Fig. 23) shows generally smooth velocities and a pre-Tertiary basement which dips gradually eastwards. Despite the smoothness of the velocity model, the reflections in the Quaternary section are quite broken and exhibit variable dips. At CDP 128000 a large velocity high corresponds to the eastern edge of a fault bound trough. Below the trough, the UPL and pre-Tertiary basement shows little disruption

suggesting strike-slip faulting and that some of the features of the trough may be the result of channelling, with a large thickness of low velocity recent infilling sediments. Further westward, reflections in the Quaternary section are broken and irregular with some suggestion of faulting identified by Johnson et al. (2000) at CDP 123700. Steep, small offset faulting at CDP 121000 (Fig. 23) cuts Quaternary and pre-Tertiary reflections and corresponds to a change in the gradient of the pre-Tertiary basement.

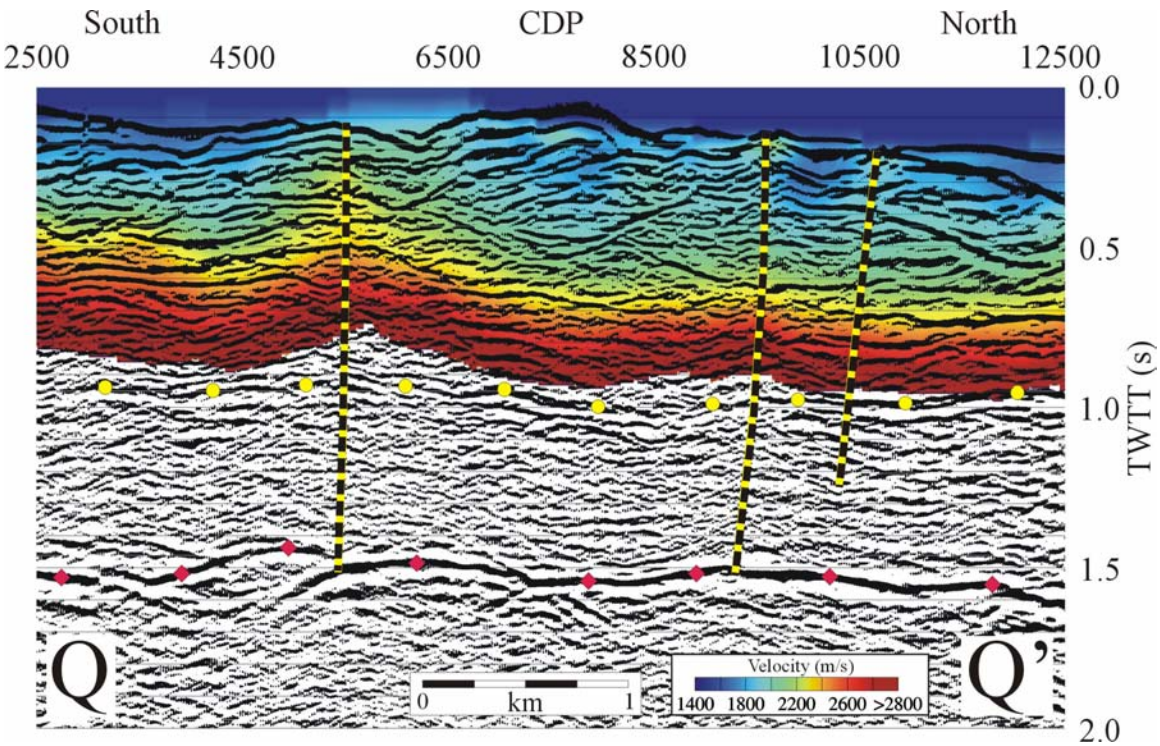

Figure 24. Section Q-Q' from seismic reflection profile JDF-4 across the NW extension of the Hood Canal -Discovery Bay fault zone. Yellow dots = UPL. Red diamonds = Pre-Tertiary basement.

Section Q-Q' (JDF-4; Fig. 24) crosses a number of the features mapped by Johnson et al. (2000) to cross section P-P' (Fig. 23). However, many of the features are greatly diminished on this more northerly profile. The fault bound trough is absent with only subtle suggestions of the associated faulting at CDP 10500. A small velocity high at CDP 9900 is associated with a fault that offsets both the pre-Tertiary basement and Quaternary section. Offsets are variable in magnitude and sense suggesting a strike-slip nature. To the south at CDP 8000 the northern edge of the bank identified in section P-P' is associated with disrupted reflections in the Quaternary section, but imaging of the fault mapped by Johnson et al. (2000) is not clear. A fault at approx. CDP 5200 shows south side up displacement of Quaternary and pre-Tertiary basement reflections by about 0.04 s TWTT. This fault, mapped by Johnson et al. (2000), is related to broken reflections at CDP 123500 on section P-P' (Fig. 23). A small (up to north) pre-Tertiary basement displacement of about 0.02 s TWTT at CDP 3000 corresponds to a pre-Quaternary fault mapped by Johnson et al. (2000). The fault is interpreted (Johnson et al. 2000) to be the

same feature at CDP 121000 on section P-P' (Fig. 23), but shows lower deformation to the northwest.

Section R-R' (SG-1; Fig. 25) crosses the northwestern extent of the HCDB fault zone according to Johnson et al. (2000). We see little evidence in velocity models, which show generally very smooth gradient, or seismic profiles to suggest a Quaternary age fault at approximately CDP 31600. However, a fault which offsets the UPL at CDP 35000 agrees well with Johnson et al. (2000) and marks the south-western end of a 1.5 km long pop-up (about 0.05 s TWTT) bound by another pre-Quaternary fault at approximately CDP 33000. The pre-Tertiary basement does not show a similar uplift, and suggests a strike-slip nature to these faults.

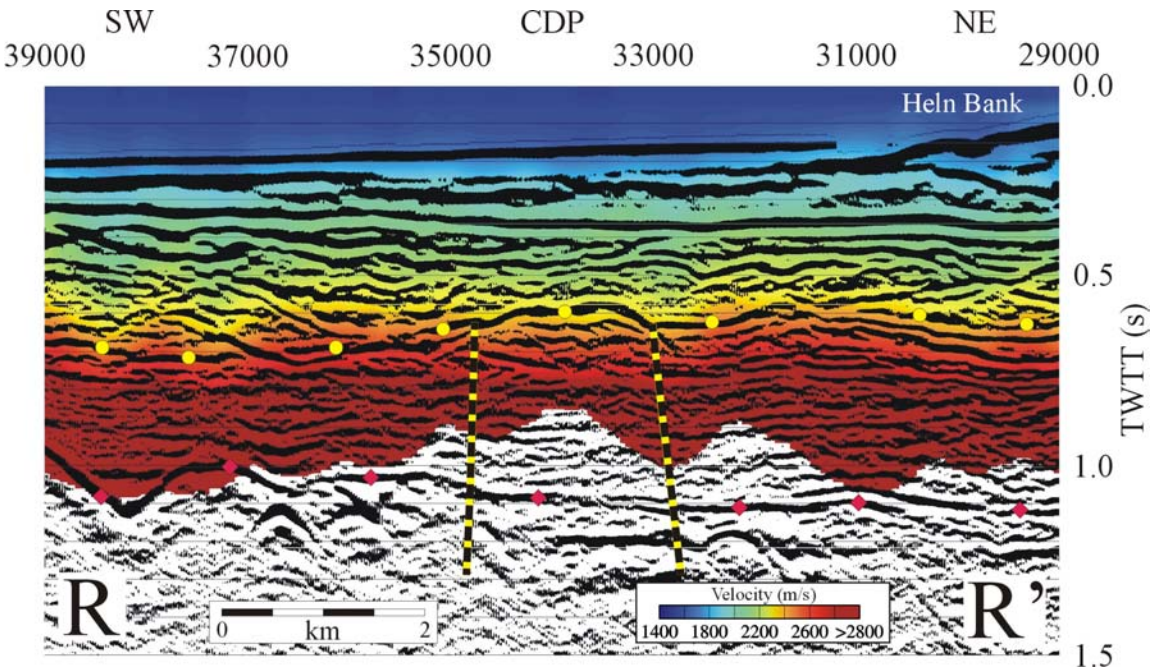

Figure 25. Section R-R' from seismic reflection profile SG-1 across the northwestern extension of the Hood Canal - Discovery Bay fault zone. Yellow dots = UPL. Red diamonds = Pre-Tertiary basement.

Immediately west of R-R', section S-S' (JDF-6; Fig. 26) shows very smooth velocities which give little indication of major faulting. At about CDP 16200 broken seismic reflections were suggested to represent Quaternary faulting (Johnson et al. 2000). The offsets are negligible and deeper units including the pre-Tertiary basement appear to be unaffected. This fault was not clearly identified on section R-R' and we suggest that if the feature does represent Quaternary faulting, the magnitude of deformation must be very small, perhaps indicating that we are, as suggested by Johnson et al. (2000), near to the end of the fault zone.

The discontinuity and variation in the magnitude and style of faults towards the northwest suggest that deformation is widely dispersed in this region and not accommodated by major continuous faults.

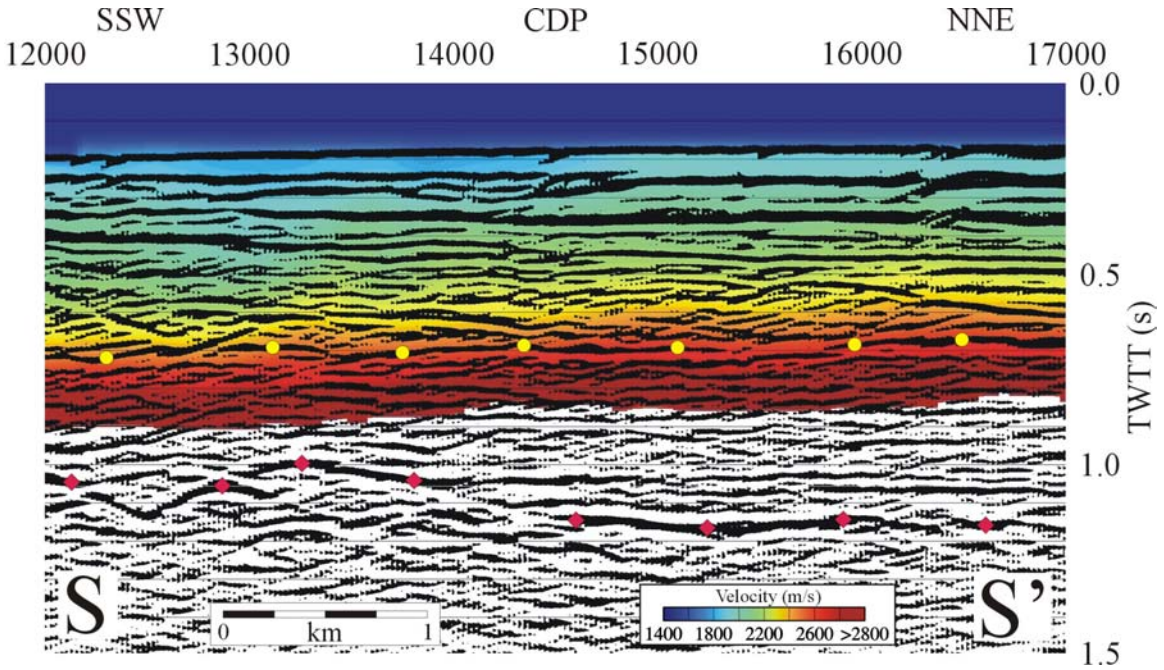

Figure 26. Section S-S' from seismic reflection profile JDF-6 across the NW extension of the Hood Canal - Discovery Bay fault zone. Yellow dots = UPL. Red diamonds = Pre-Tertiary basement.

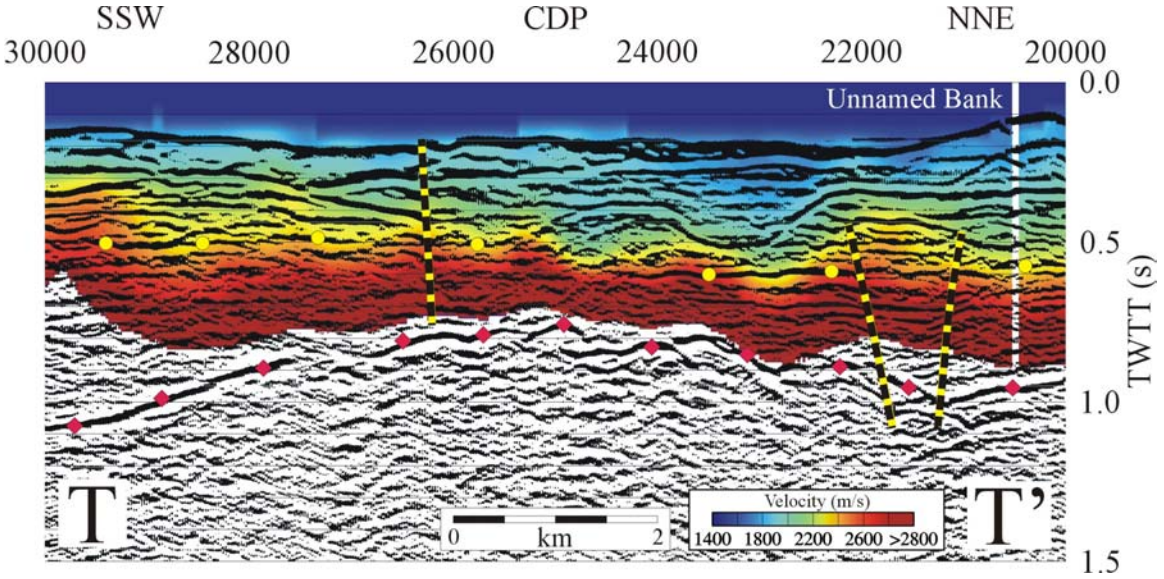

Figure 27. Section T-T' from seismic reflection profile JDF-5 west of the HCF zone. Yellow dots = UPL. Red diamonds = Pre-Tertiary basement.

5.3.2. Faulting in the southwestern corner of the E. Strait of Juan de Fuca

Several faults, of a similar orientation to the northwestern extension of the HCDBF zone, have been identified (Johnson et al. 2000) to the west. Section T-T' (JDF-5; Fig. 27) crosses a number of these features and shows them to be associated with deflections in the velocity model. Higher velocities (>2200 m/s) and velocity gradients along this profile appear to be associated with an unconformity within the Quaternary section which has been infilled by flatter lying more recent sediments.

From approximately CDP 21300 - 22600 a broad velocity high within the Quaternary section relates to two steeply inward dipping faults that bound a slightly uplifted (~0.02 s TWTT) pop-up. The pre-Tertiary basement shows a change from apparent SSW dipping continuous reflections to NNE dipping reflections below. Further to the SSW, velocity anomalies at approximately CDP 26300, 27600 and 29100 may be related to Quaternary faulting identified by Johnson et al. (2000). Although the Quaternary section shows numerous irregular and broken reflections, the only clear reflection offset associated with these features is observed at CDP 26300. Another similar high at CDP 25400, related to broken Quaternary reflection may also indicate additional small offset faulting. All of these features lie atop of a pre-Tertiary basement high whose reflection are broken and irregular.

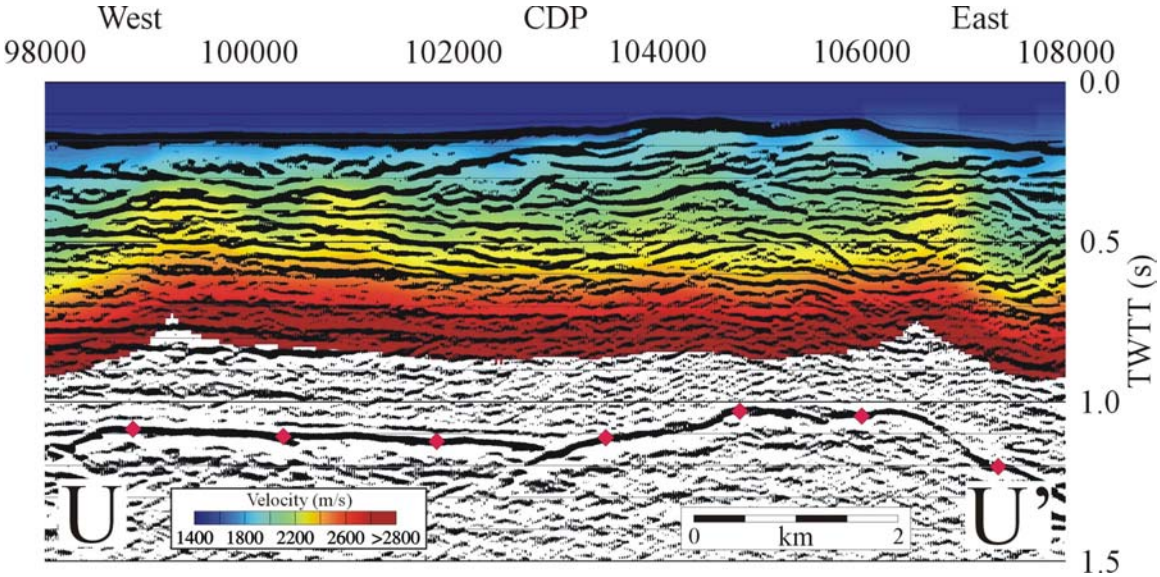

Figure 28. Section U-U' from seismic reflection profile JDF-2 west of HCF zone. Red diamonds = Pre-Tertiary basement.

A number of the features suggested for section T-T' are also crossed to the southeast by section U-U' (JDF-2; Fig. 28). Quaternary faults were interpreted by Johnson et al. (2000) at CDP 100000, 102100, 103900 and 105900. Broken and irregular reflections are observed in the Quaternary section above 0.6 s TWTT and suggest that faulting, as with section T-T', is more complicated than previously interpreted. Reflections in the pre-Quaternary section below 0.6 s TWTT, are generally continuous, fairly flat lying and

between CDP 98000 - 103000 are parallel to the prominent pre-Tertiary basement reflection. Between CDP 103000 - 107000 pre-tertiary basement relief of over 0.1 s TWTT is accompanied by deformed reflections in the pre-Quaternary section.

6. Discussion and Conclusions

Tomographic velocity models have significantly aided in the interpretation of faults in the Eastern Strait of Juan de Fuca. Seismic reflection profiles suggest that primary pre-Quaternary motion on the Devils Mountain fault to the east of 122.95° W was transferred to faulting identified on profiles PS-2 (E-E'; Fig. 11) and SG-1 (F-F'; Fig. 12) marked by a large fault scarp. We believe that the fault scarp here identified is related to a westward extension on the Utsalady Point fault, which shows a similar (G-G'; Fig. 13), although slightly smaller scarp west of Whidbey Island. This agrees with the results of Johnson et al. (2001) who suggest that the UPF and SPF represent major active structures. The connection between the western section of the DMF and the implied western extension of the UPF is difficult to access due to the lack of seismic profiles in this region, but it appears to step to the south. This may be due to antithetic or en-echelon faulting associated with the DMF zone. More recent deformation has clearly been experienced on the eastward continuance of the DMF, which east of 122.95° W affects a shallow pre-Tertiary basement and thin overburden far north of the primary fault scarp. However, Quaternary deformation associated with the primary fault scarp appears to be of as significant a magnitude as faulting on the DMF to the northeast.

The Southern Whidbey Island fault shows a character common of transpressional faults, with steep faults exhibiting changes in the sense reflection offsets with depth and a great variation in dips and structure along strike. As with the Southern Whidbey Island fault, faults in the south-western corner of the Eastern SJDF show a complicated pattern of small offset en-echelon faults whose magnitude deceases towards the northwest.

7. References

Aldridge, D.F., and Oldenburg, D.W. 1993. Two dimensional tomographic inversion with finite difference traveltimes. Journal of Seismic Exploration, 2, 257-274.

Atwater, B., and Moore, A.W. 1992. A tsunami about 1000 years ago in Puget Sound. Science, 1614-1616.

Booth, D.B. 1994. Glaciofluvial infilling and scour of the Puget Lowland, Washington, during ice-sheet glaciation. Geology, 22, 695-698.

Brocher, T.M., Parsons, T. Blakely, R.J., Christensen, N.I., Fisher, M.A., Wells, R.E, and the SHIPS Working Group. 2001. Upper crustal structure in Puget Lowland, Washington: Results from the 1998 Seismic Hazards Investigation in Puget Sound. Journal of Geophysical Research, 106, B7, 13541-13564.

Calvert, A., Fisher, M., Cleary, M., Mosher, D., Hyndman, R., Brocher, T., and SHIPS Working Group. 2000. Tomographic Imaging of Shallow Faulting in the Strait of Georgia using SHIPS Reflection Data. EOS Transactions of the American Geophysical Union, F878.

Christie-Blick, N., and Biddle, K.T. 1985. Deformation and basin formation along strike-slip faults, *in* Biddle, K.T., and Christie-Blick, N., eds., *Strike-Slip Deformation, Basin Formation, and Sedimentation:* Society of Economic Paleontologists and Mineralogists Special Publication No. 37, p. 1-34.

Fisher, M.A., et al. 1999. Seismic survey probes urban earthquake hazards in Pacific northwest. EOS Transactions of the American Geophysical Union, 80, 2, 16-17.

Gower, H.D., Yount, J.C., and Crossen, R.S. 1985. Seismotectonic map of the Puget Sound region, Washington. U.S. Geological Survey. Misc. Invest. Ser. map, I-1613.

Johnson, S.Y., Dadisman, S.V., and Mosher, D.C. 2001. Active tectonics of the Devils Mountain Fault and related structures, northern Puget Lowland and eastern Strait of Juan de Fuca region, Pacific Northwest. U.S. Geological Survey Prof. paper 1643.

Johnson, S.Y., Mosher, D.C., Dadisman, S.V., Childs, J.R., and Rhea, S.B. 2000. Tertiary and Quaternary structures of the eastern Juan de Fuca Strait: interpreted map. *In: Mosher, D.C., and Johnson, S.Y. 2000. Neotectonics of the eastern Juan de Fuca Strait: a digital geological and geophysical atlas. Geological Survey of Canada Open File report 3931.*

Johnson, S.Y., Dadisman, S.V., Childs, J.R., and Stanley, W.D. 1999. Active tectonics of the Seattle fault and central Puget Sound, Washington - Implications for earthquake hazards. Geological Society of America Bulletin, 111, 7, 1042-1053.

Johnson, S.Y., Potter, C.J., Armentrout, J.M., Miller, J.J., Finn, C., and Weaver, C.S. 1996. The southern Whidbey Island fault, an active structure in the Puget Lowland, Washington. Geological Society of America Bulletin, 1098, 334-354 and oversize insert.

MacLeod, N.S., Tiffen, D.L., Snavely Jr., P.D., and Currie, R.G. 1977. Geological interpretation of magnetic and gravity anomalies in the Strait of Juan de Fuca, U.S. - Canada. Canadian Journal of Earth Sciences, 14, 223-238.

Mazzotti, S., Dragert, H., Hyndman, R.D., Miller, M.M., and Henton, J.A. 2002. GPS deformation in a region of high crustal seismicity: N. Cascadia forearc. Earth and Planetary Sciences Letters, 198, 41-48.

Miller, M.M., Johnson, D.J., Rubin, C.M., Dragert, H., Wang, K., Qamar, A., and Goldfinger, C. 2001. GPS-determination of along-strike variation in Cascadia margin kinematics: Implications for relative plate motion, subduction zone coupling, and permanent deformation. Tectonics, 20, 2, 161-176.

Mosher, D.C., and Johnson, S.Y. 2000. Neotectonics of the eastern Juan de Fuca Strait: a digital geological and geophysical atlas. Geological Survey of Canada Open File report 3931

Oldow, J.S. 2000. Fault Characterisation and assessment of slip on the Devil's Mountain and North Whidbey Island fault systems, northwestern Washington. USGS Technical Report 276.

Pratt, T.L., Johnson, S., Potter, C., Stephenson, W., and Finn, C. 1997. Seismic reflection images beneath Puget Sound, western Washington State: The Puget Lowland thrust sheet hypothesis. Journal of Geophysical Research, 102, 27469-27489.

Roberts, T.H. 1991. Gravity investigation of crustal structure in the eastern Olympic Peninsula-Puget Lowland area, Washington. Masters Thesis, Western Washington University, Bellingham, WA, United States.

Weaver, C.S. and Smith, S.W. 1983. Regional Tectonic and Earthquake Hazard Implications of a Crustal Fault Zone in Southwestern Washington. Journal of Geophysical Research, 88, B12, 10371-10383.

8. Bibliography

Hayward, N., Nedimovic, M., Cleary, M., Mosher, D.C., and Calvert, A. 2003. Composite Tomographic and Reflection Images of Potentially Active Faults in the Eastern Strait of Juan de Fuca, Western Canada. Geological Society of Canada Meeting. Vancouver May 25-28.

Mosher, D.C., Johnson, S.Y., Nedimovic, M. and Hayward, N. 2003. Fault recognition and active tectonics in the eastern Juan de Fuca Strait, Cascadia forearc region. Geological Society of Canada Meeting. Vancouver May 25-28.